"Two-Channel Electronically Tunable Integrated Optical Waveguide Coupler On SOI"

Dissertation submitted in the partial fulfilment of requirement for the award of degree of

Master of Engineering

In

Electronics and Communication Engineering

Submitted by:

Rohit Choudhary

(801161023)

Under the guidance of:

Dr. Mukesh Kumar

ELECTRONICS AND COMMUNICATION ENGINEERING DEPARTMENT

THAPAR UNIVERSITY

(Established under the section 3 of UGC Act, 1956)

PATIALA – 147004 (PUNJAB)

JULY-2013

DECLARATION

I **Rohit Choudhary**, hereby declare that the work which is being presented in this dissertation entitled **"Two-Channels Electronically Tunable Integrated Optical Waveguide Coupler On SOI"** by me in partial fulfilment of the requirement for the award of degree of Master of Engineering in Electronics and Communication Engineering from Thapar University, Patiala, is an authentic record of my own work carried out under the supervision of **Dr. Mukesh Kumar**

The matter presented in this thesis has not been submitted in any other university/institute for the award of any other degree.

Date: 12-7-13

"Rohit Choudhary"

(801161023)

It is certified that the above statement made by the student is correct to the best of my knowledge and belief.

Date: 12-7-13

"Dr. Mukesh Kumar"

Assistant Professor, ECED

Countersigned by:

"Dr. Rajesh Khanna"

Professor and Head ECED

Thapar University, Patiala

"Dr. S.K. Mohapatra"

Dean of Academic Affairs

Thapar University, Patiala

ACKNOWLEDGEMENT

I would like to express my special thanks and deep sense gratitude to my Dissertation Advisor, **Dr. Mukesh Kumar**, Assistant Professor, Electronics & Communication Engineering Department, Thapar University, Patiala for their continuous indefatigable guidance, which paved me on to the path to carry this project. He has always been very encouraging and offered invaluable advice. I am highly indebted to them for their painstaking efforts and invaluable suggestions during the period of work.

I am also thankful to **Dr. Rajesh Khanna**, Professor and Head and **Dr. Kulbir Singh**, Associate Professor, Electronics & Communication Engineering Department, Thapar University, Patiala for their valuable advice and helped in all possible ways for the completion of my thesis work.

I wish to express thanks to all those persons who with their encouraging words and suggestions have contributed directly or indirectly for the completion of this work.

ABSTRACT

Integrated electro-optic waveguide coupler is a potential candidate for telecommunication systems which provides a promising platform to realize integrated waveguide devices. High speed active waveguide devices which may include optical switches and modulators have been a challenging subject in modern integrated optics. In an effort to move this important issue along, this work mainly focuses on concepts of improving the self-imaging quality of wave guide coupler in terms of coupling length analysis. Optical waveguide couplers have been comprehensively studied over the years due to its diverse application in the systems of time division multiplexing space division multiplexing and wavelength division multiplexing. Recently the high speed silicon waveguide coupler, one of the key component for integrated Si photonic chip are used to transmit *Tb/s* data over the communication link and attracted a lot of attention for next generation communication network as well as high performance computing applications.

To decrease the coupling length of high speed active waveguide devices, an electronically tunable waveguide coupler based on carrier plasma dispersion effect incorporating silicon on insulator rib waveguide is proposed. Silicon-on-insulator (SOI) optical waveguides have emerged as an attractive class to design advanced low-power, high-speed opto-electronic devices. The design of the wave guide coupler is presented by optimizing the various device parameters, such as waveguide width (w), height (h) and gap (g) between the waveguides to obtain shortest switching length at small power. Design and simulation of such structure is performed with finite difference method. By varying the separation between the wave guides partial image and complete image has been formed at gap $0.05\mu m$ and $0.07\mu m$ respectively. Coupling lengths for partial image and complete image are reported $7.7\mu m$ and $27.48\ \mu m$ respectively in simulation at 1 volt. Reduction in coupling length of about 4 times and 1.06 times for partial images and complete images respectively are achieved from 0 volt to 1 volt. Thus tuning of waveguide coupler in this way provides a promising approach for enabling high speed sub-micron size active waveguide devices on Si and it can also offer the multi channel waveguide coupler for applications in WDM systems.

Table of Contents

LIST OF FIGURES

Chapter 1

Introduction to integrated photonic devices

1.1 Background

Optical communication is one of the greatest successes people achieved in the last century. It provides an excellent solution for the flow of information. The explosive expansion of Internet services has led to a transformation from “telecommunication” to “data communication”. The digital data traffic has been doubling every half-year. To support this revolution, fiber-optic communication technologies have developed rapidly because it could offer much higher speed and larger capacity [1, 2]. The twisted-pair and coaxial-cable are being replaced by fibers gradually [3]. After the long distance fibers have been settled, the choke point of the optical communication system is moving to functional integrated photonic components which are used to connect the terminals and the customer.

Integrated optics refers to the implementation of various functions with light such as generation, modulation, switching, and detection in an optical guided wave structure formed on a single substrate [4, 5]. Over the past decade, integrated optics devices have revolutionized communications. Tremendous advancement in Optical Integrated Circuit (OIC) technology has taken place in recent times and era of All Optical Networks (AON) is about to dawn. As far as optical communications is concerned, crudely there are certain stages of evolution that can be discerned. Stage one of fiber-optic development can probably be considered mature. These links typically consists of directly modulated source, pigtailed into the fiber, and with the signal detected on a photodiode only by its amplitude variance. Stage two can perhaps be considered as the present day, where more sophisticated requirements have to be addressed, and the simple laser-fiber-detector system is not necessarily suitable for the task. It is in this second stage of development that the unique properties of integrated optics devices are beginning to play a greater role in improving the performance of fiber-optic communication systems. In the next stage of technological advancement, the integrated optical waveguide coupler use as switch matrices, multiplexers, de-multiplexers, acousto-optic tunable filters, modulators and

switches [6] etc. have made Wavelength Division Multiplexing (WDM), Dense Wavelength Division Multiplexing (DWDM) and Coarse Wavelength Division Multiplexing (CWDM) networks feasible. Integrated optics devices consist of dielectric waveguides that constitute the optical paths analogous to the conductor paths of microelectronics. These structures are small ribs or stripes with cross-section dimensions of the order of μm's fabricated by thermal diffusion of transition metals, ion implantation, etching techniques or proton-exchange from stacks of transparent dielectric films, etc. Similar to optical fibers, they are able to confine, i.e. 'guide' light via the mechanism of total internal reflection (TIR) [7]. Several material technologies have emerged for fabricating integrated optic devices. The use of silicon for optical interconnects would enable a platform for a monolithic integration of optics and microelectronics [8, 9]. Photonics on silicon has been suggested since the 1980s. SILICON as a photonic medium has unique advantages. It is transparent in the range of optical telecommunications wavelengths (1.3 and 1.55 m) and has a high index of refraction, which allows for the fabrication of high-index-contrast sub micrometer structures [10].

1.1.1 Features of Optical Integrated Circuits (OIC)

Optical IC can be broadly classified into three types i.e. monolithic, hybrid or quasi-hybrid. When three basic components i.e. source, waveguide, and detector are all integrated on a single substrate, the device is called a monolithic optical IC. Compound semiconductors from group III-V, such as GaAs and InP, can be the probable choice of substrate for these optical IC's. Though, this may not necessarily be the best material for a particular device. This leads to degradation of the overall system performance. In the hybrid optical IC's, all the three components are made of different materials. i.e. Source, waveguide, and detector are made of compound semiconductor and dielectric materials, such as glass or $LiNbO_3$, and Silicon (Si) respectively [11-13]. Lastly, quasi–hybrid Optical IC is an intermediate between the monolithic and hybrid IC's. Features of integrated optics devices are:

(a) Features based on wave optics: Devices consist mainly of single-mode waveguides with widths of the order of *μm's* and in which a single-mode optical wave propagates. These optical devices can be treated by wave optics.

(b) Stable alignment by integration: Assembly problems in OIC are less since several discrete components can be integrated on a single substrate. Optical axis adjustment and precise positioning are not necessary, and stable alignment is maintained.

(c) Easy control of guided wave: It is easier to control guided waves by electro-optic effects, acousto-optic effects and thermo-optic effects. Since waveguides are of the single-mode type [14, 15].

(d) Low operating voltage and short interaction length: Because of single- mode waveguide construction, gaps in controlling electrodes can be reduced. Consequently, low operating voltage is possible [16]. Also, as interaction increases, the interaction length becomes shorter, making the devices more compact.

(e) Faster operation: A shorter electrode length and less capacitance makes switching and modulation speed faster [7, 11].

(f) Compact and light weight: Since several components are integrated on a thin substrate of a few square centimeters, these devices are quite compact and light in weight [17].

(g) Low price: The development of integration techniques has made the mass production possible, and has reduced the amount of materials needed. The possibility of lower prices [18] in the future, therefore, is very real.

As we see that Si based integrated optic technology [8, 9, 13] is making a revolutionary change in the field of the optical communication. Broadband networks providing various kinds of services have been receiving increasing attention in recent years. To realize such networks, both broadband transmission and switching system are required. Application of photonic technologies is promising in achieving such broadband transmission and switching systems. One of the most attractive features of photonic technologies is its capability of making full use of wavelength domain. More than 30 THz bandwidth can be utilized by making full use of the low loss region of single mode optical fibers, which extends from 1.3 to 1.6 μm. By directly utilizing this wavelength region, Wavelength-Division-Multiplexing (WDM) transmission can increase the capacity without any

limitation imposed by the electronic circuit operation and its key elements are guided wave optical devices.

In this chapter, a general idea of integrated guided-wave optical devices is given. After an overview of different guided wave optical devices, a short introduction of the goal and outline of this work is given.

1.2 Guided-wave Integrated Optical Devices and Application

Guided-wave optics has important applications in directing light to awkward places, in establishing secure communications, and in the fabrication of miniaturized optical and optoelectronic devices that requiring the confinement of light. There is now little doubt that guided wave optical devices will have an increasing impact on electrical engineering in the coming years. Primarily, this is due to the sustained development of two extremely successful components: optical fibre and the semiconductor laser [19]. Together, these are currently in the process of revolutionising the telecommunications industry, and making considerable advances in a variety of other new and exciting application areas.

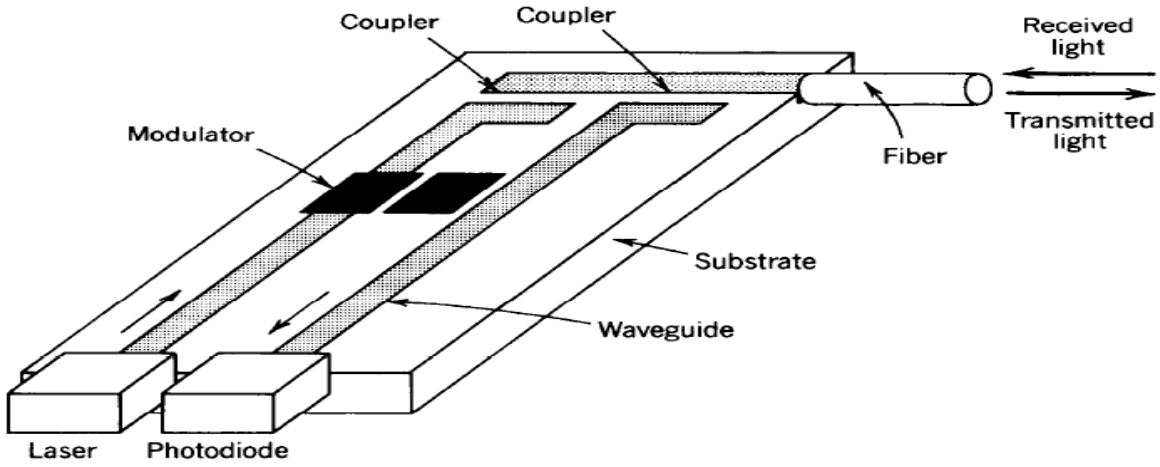

Fig: 1.1 An example of an integrated-optic device used as an optical receiver/transmitter. Received light is coupled into a waveguide and directed to a photodiode where it is detected. Light from a laser is guided, modulated, and coupled into a fiber [20].

Integrated optics is the technology of integrating various optical devices and components for the generation, focusing, splitting, combining, isolation, polarization, coupling, switching, modulation and detection of light, all on a single substrate (chip) [20]. Optical waveguides provide the connections between these components. Such chips (as shown in Fig: 1.1) are optical versions of electronic integrated circuits.

It is clear from above Fig. that the basic components of guided wave devices are optical coupler [21]. In its simplest form, this acts as a beam splitter, but more complicated devices can be used as two-way switches or modulators and mux/dmux [22, 23]; which are as follow-

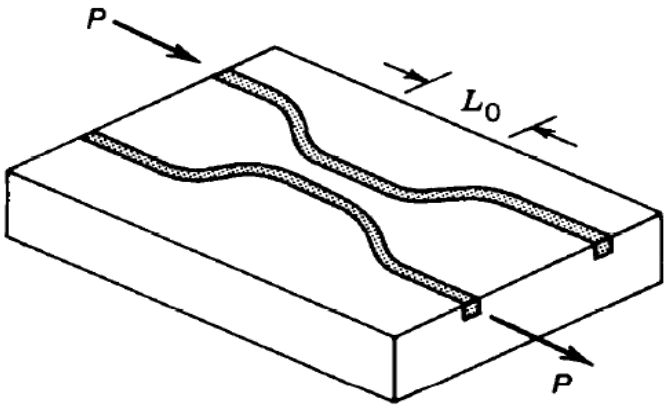

Fig: 1.2 Simplest form of integrated optical coupler [19].

1.2.1 Demultiplexer/Multiplexer

The mostly used guided wave devices for Demux/Mux in single mode WDM system are a wavelength selective directional coupler. A multichannel Demux/Mux [24] can be realized by cascading such couplers but long length of these couplers limit the number of channels. To reduce this problem, another type of Demux/Mux which uses the wavelength dependent Two-Mode Interference (TMI) is realized. In TMI Demux/Mux, the channel tuning can be achieved by varying the branching angle or slightly variation of two mode section length and electrode voltage.

1.2.2 Optical Switch

The optical switches are generally based on electronically controlled optical directional couplers. The base material of these devices is a ferroelectric, crystalline material known

as lithium niobate, Si possessing excellent optical and electro optical properties [21]. Thus, the material's properties namely its dielectric and refractive index, can be predictably and repeatedly manipulate by applying voltage. This type of switches is generally called electro optic switches. These switches are more reliable and faster than micro-electro mechanical switches as their switching time is in nanoseconds [25].

1.3 Optical Waveguides

All optical systems rely on devices that can transmit and manipulate optical power. In the case of integrated optic systems, these objectives have been achieved by means of thin film dielectric waveguides [26]. An optical waveguide is a light conduit consisting of a slab, strip, or cylinder of dielectric material surrounded by another dielectric material of lower refractive index. The light is transported through the inner medium without radiating into the surrounding. The most widely used of these waveguides is the optical fiber, which is made of two concentric cylinders of low-loss dielectric material such as glass. Any optical power that gets coupled to the region of higher refractive index gets confined within the waveguide and travels through the substrate in the form of guided modes. The mode(s) propagating through the waveguide are solutions of the Maxwell's propagation equation

$$\nabla^2 E(r) + k^2 n^2 E(r) = 0 \qquad 1.1$$

Subject to continuity of E and H fields at the interfaces and suitable dimensions of the waveguide. The waveguide structures have been theoretically subdivided into planar waveguides and channel waveguides.

1.3.1 Planar Waveguides

A planar dielectric waveguide is a slab of dielectric material surrounded by media of lower refractive indices. The light is guided inside the slab by total internal reflection. In thin-film devices the slab is called the "film" and the upper and lower media are called the "cover" and the "substrate," respectively. The inner medium and outer media may also be called the "core" and the "cladding" of the waveguide, respectively. The propagation of light in a symmetric planar dielectric waveguide made of a slab of width d

and refractive index n, surrounded by a cladding of smaller refractive index n_c, as illustrated in Fig. 1.3. In planar waveguide the confinement of light energy is only along one transverse dimension and the light energy can diffract in other transverse plane [7, 19].

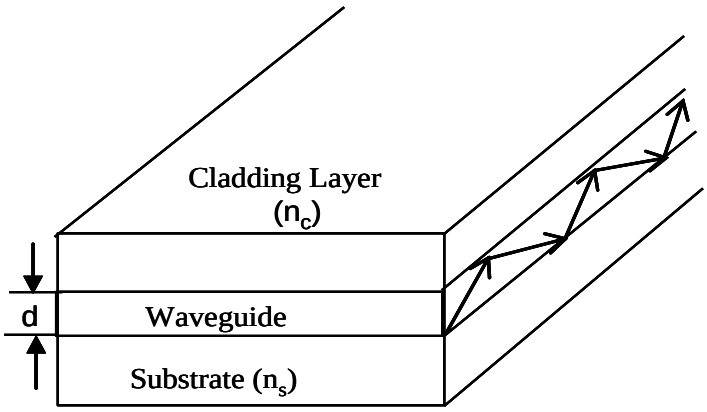

Fig: 1.3 Planar waveguide [19].

1.3.2 Channel Waveguides

A channel waveguide is formed from a slab waveguide composed of a core material and surrounded by a cladding/buffer material of lower refractive index ridge and the strip-loaded waveguides illustrated in Fig. 1.4.

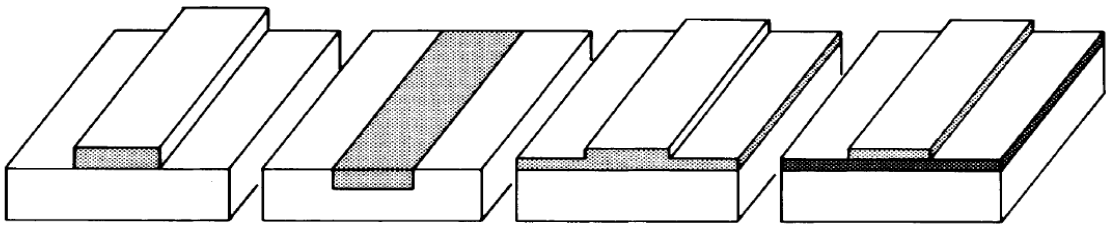

(a) (b) (c) (d)

Fig: 1.4 Various types of Channel waveguide geometries: (a) strip; (b) embedded strip; (c) rib or ridge; (d) strip loaded. The darker the shading, the higher the refractive index [27].

In contrast to planar waveguide channel waveguide confine the light energy in both transverse dimension this confinement is the desirable feature for the fabrication of devices such as modulators, and couplers.

The analysis of a channel guide is generally a complicated problem, and different approaches are used channel waveguides. Since the index changes concerned in the former are so large, a TEM model cannot be used, and a rigorous solution is normally required. Fig: 1.4 shows one possible model of a ridge guide, which consists of a region of dielectric of rectangular cross-section surrounded by regions of differing refractive indices.

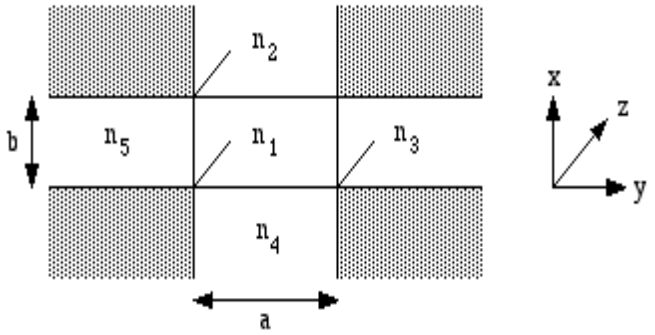

Fig: 1.5 Model of a rectangular dielectric waveguide [7].

It has been shown that modes of such a guide can be found (at least approximately) by assuming solutions for the transverse variation of the electric field in the form of a product, i.e. as $E_T(x, y) = E_1(x)\, E_2(y)$. Since the layers are individually uniform, we may guess that $E_1(x)$ and $E_2(y)$ must have the form either of cosinusoidal or of exponential functions, by analogy with the solution for a slab guide. These solutions are then built up in a piecewise fashion, as follows:[7, 27]

In Region 1, the field is assumed to vary cosinusoidally with both x and y. In Region 2, the field is assumed to decay exponentially with x, and vary cosinusoidally with y In Region 3, the field is assumed to vary cosinusoidally with x, and decay exponentially with y and so on. These fields are matched rigorously at the interfaces between Regions 1 and 2, 1 and 3, 1 and 4, and 1 and 5, but only approximately in the shaded corner regions. The result is a set of two- dimensional mode patterns, which are neither truly TE nor truly

TM. Often, the confinement provided by the layering is much stronger than that in the lateral direction, so this type of mode may be non-circular, with a high aspect ratio.

1.4 Motivation and Goal of This Work

Data transmission can be the limiting factor in certain fields. For example, large data centers, server farms or super computers need to transmit a massive amount of data between chips and other banks and are becoming increasingly dependent on ultra-fast data transfer. While it is possible to still do this with physical electrical connections, high speed optical interconnects are being seen as a promising technology. The evolution of fiber optics communications with its emphasis on high-data rate single-mode fiber networks using 1.3µm -1.6µm wavelength region and on sophisticated optical systems has stimulated the applications of guided wave devices. Integrated optics which basically uses single-mode guided wave techniques, contributes to rugged, cost effective and batch-fabricated components such as modulators/switches, demultiplexers, multiplexers, tunable filters, frequency shifters, polarization controllers, signal routing and timing devices. The functions of these devices can be realized by using the electro-optic waveguide components. The mature Si integrated circuit technology enables the implementation of dense silicon-based integrated optics and electronics on-chip. In order to achieve low-loss compact (sub micrometer size) devices, high refractive index contrast is required. For this purpose, silicon-on-insulator (SOI) waveguide technology may be employed. Very little work has been reported on high-index-contrast (high lateral optical confinement) waveguide active devices despite their high demand to manipulate light beams for information processing (e.g., coding–decoding, routing, multiplexing, timing, logic operations, etc.) in high-density integrated- optic circuits. This project centers on optimizing a single component of an optical system designed to transmit data at extremely high speeds. The component we are attempting to design and optimize is a Electro-optic waveguide coupler, which will be used as an optical switch which couple the power between the waveguides at very small switching length. . Ultimately, it will be used as modulators and other active optical devices in ultra-fast wavelength division multiplexing and de multiplexing applications. The motivation behind this project is to design a SOI configuration that will act as a waveguide coupler, i.e. to design a device that that will couple the power between the waveguide at different applied voltage across

the device. The characteristics of this electro-optic waveguide coupler will determine the minimum coupling length between the waveguide at different applied voltage

1.5 Outline of Dissertation

The scope of this work is the design of electro-optic waveguide coupler based on MMI and self imaging principal. The purpose of our research is to improve the coupling in terms of coupled power and coupling length of conventional waveguide coupler. Focus of the work will be on SOI structure. The work is organised as follow

Chapter 2, focus on the basic principles and physics relevant for understanding of electro-optical waveguide coupler. First theoretical model of waveguide coupler are presented. Subsquently a detailed description of the properties of electro optic effects in terms pockel effect, Kerr effect, Franz Keldysh and carrier plasma effect are explained. After that SOI based coupler is introduced.

Chapter 3 gives the summery of literature survey

Chapter 4, proposed the design of electronically tunable waveguide coupler based on carrier plasma dispersion effect. The detailed description of complete image and partial image theory are given. Furthermore the simulation results are outlined in this chapter.

Chapter6 summarizes the achievements of this work.

Chapter 2

Electro-optic waveguide coupler

2.1 Introduction

Optical wave guide coupler is a key component in optical telecommunication systems, with applications in the systems of time division multiplexing, space division multiplexing and wavelength division multiplexing [24]. In chapter 1, we have start with one of the most successful and versatile devices in both integrated and fibre optics, the waveguide coupler, which works by coupling the modes travelling in the same direction. In its simplest form, this acts as a beam splitter [28, 29], but more complicated devices can be used as two-way switches or modulators [15, 23]; further variants can be used as filters or polarizer. However, such structures have their flow of light predetermined by the design of the structure and cannot be modified once fabricated. In order to control the flow of light in modulators and switches A field is applied across the device which modifies its effective refractive indices. This change in the effective refractive index induces a change in the transmission properties of the device [30].

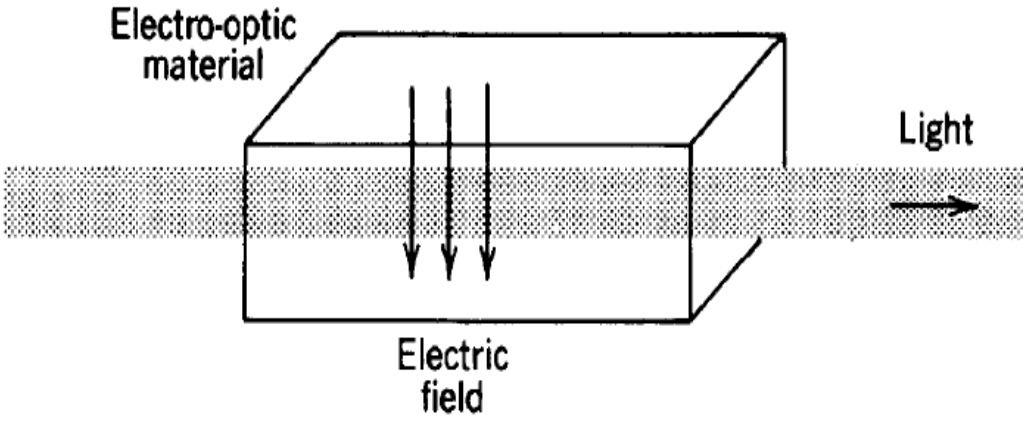

Fig: 2.1 A steady electric field applied to an electro-optic material changes its effective refractive index. This in turn, changes the effect of the material on light trave--lling through it. The electric field therefore controls the light [30]

This chapter gives a detailed description of the principles and the physics of optical waveguide coupler and In order to discuss the dependency of electric field on waveguide coupler with the application of voltage, different models of electro optic effect ("free carrier dispersion effect, the Pockel effect and the Franz-Keldysh effect) are presented.

2.2 Waveguide Coupler Theory

Guided mode has fields extending beyond the guiding region into the surrounding medium [31], decaying exponentially as one moves far from the waveguide boundary. If one brings two such waveguide close together so that the evanescent fields of the propagating modes in the two waveguide overlap, then there is a coupling between the two waveguides. When guides are placed sufficiently close together, these parts of the field must overlap spatially. Usually, the inter waveguide gap required for this overlap to be significant is of the order of the guide width. So exchange of power between guided modes of two parallel waveguides is known as directional coupling. It is anticipated that waveguide directional couplers will perform a number of useful functions in thin-film devices, including power division, modulation, switching, frequency selection, and polarization selection.

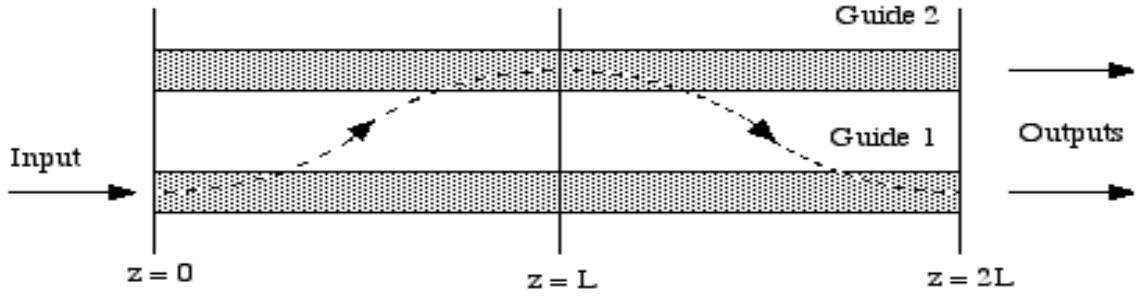

Fig: 2.2 Conceptual representation of the coupling process [31]

From Fig: 2.2 the input is to Guide 1, at z = 0. We shall assume that complete coupling occurs at z= L, when all the light has been transferred to Guide 2. At z = 2L, therefore, the light will have been completely coupled back to Guide 1, and so on. In fact, the process is a continuous, bidirectional one, of a type known as multiple scattering. The condition the guides must satisfy for 100% power transfer is therefore that they are synchronous (i.e. have the same propagation constants) [23] so that all the scattered contributions add up in-phase. This usually requires them to be identical [32].

Fig: 2.3 show a waveguide coupler consisting of two waveguide which are in close proximity over a length L if energy is incident on one of the waveguide then there is a periodic exchange of energy between the two waveguide. If the propagation constant of the mode in the two wave guide are identical then there is a complete transfer of energy from one waveguide to other.

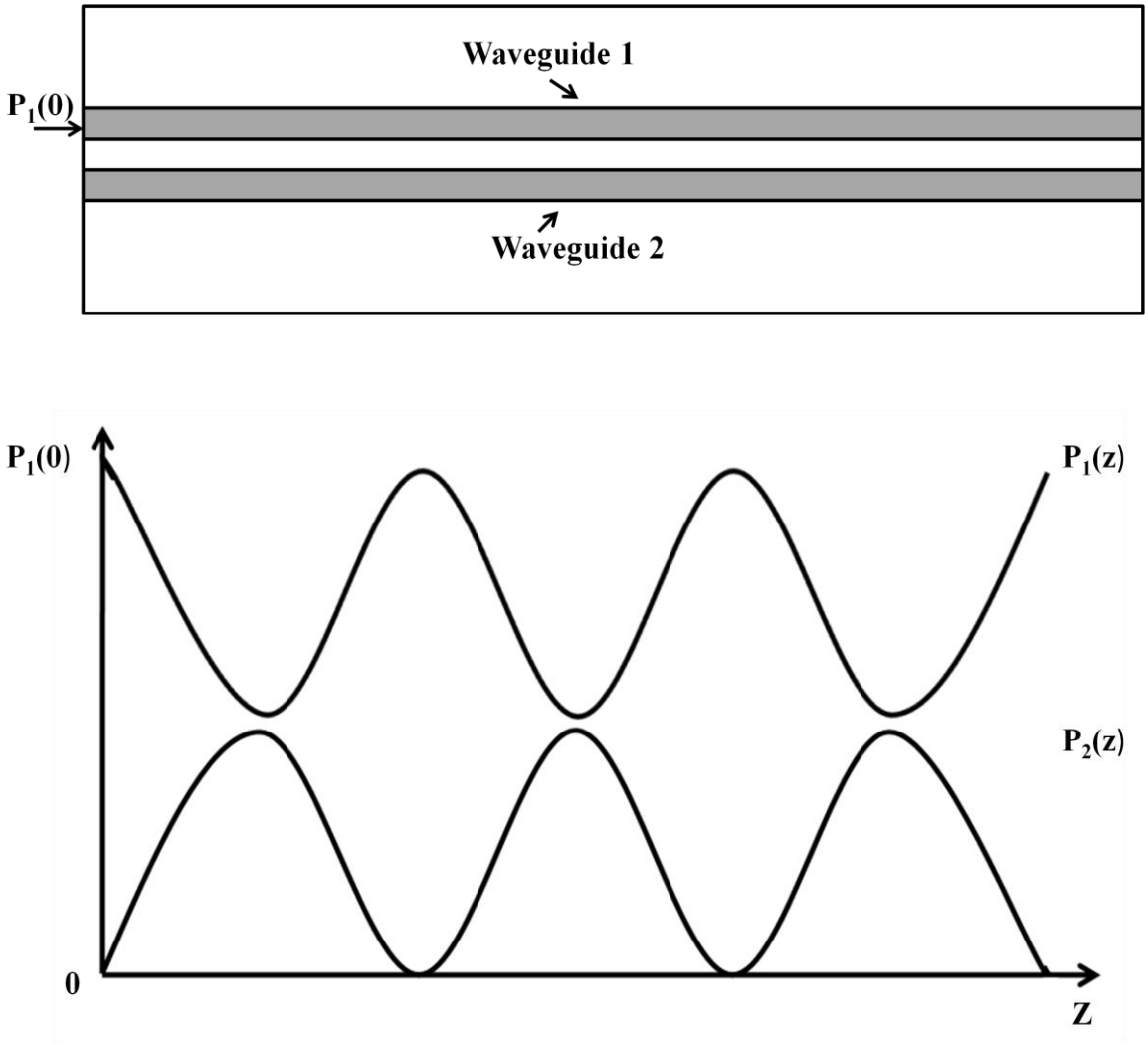

Fig: 2.3 Periodic exchange of power between guides 1 and 2. [33]

The modal field of single waveguide varies with z in the form of $e^{-i\beta_1 z}$ and hence the amplitude of mode at z as a(z) [33]

$$da/dz = -i\beta_1 a \quad (2.1)$$

Here β_1 is the propagation constant of the mode in the waveguide 1. Similarly if b(z) represent the amplitude at z of a mode in waveguide 2 with propagation constant β_2

$$db/dz = -i\beta_2 b \quad (2.2)$$

Equation 2.1 and 2.2 are valid when waveguide 1 and 2 are non interacting. When two waveguide are close together then the modes in the two wave guide can interact through the evanescent field. So the variation of amplitude of the modes in two waveguide

$$da/dz = -i\beta_1 a - ik_{12} b(z) \quad (2.3)$$

$$db/dz = -i\beta_2 b - ik_{21} a(z) \quad (2.4)$$

Where the constant k_{12} and k_{21} represent the strength of interaction between the two modes and are referred to as coupling constant. The coupling constant depends upon the waveguide parameters, such as separation between the waveguides and the wavelength of operation. In order to solve the equation 2.1 and 2.2 we postulate the existence of a wave in the system consisting of the two coupled waveguide, which propagate with a phase constant β

$$a(z) = a_0 e^{-\beta z} \quad (2.5)$$

$$b(z) = b_0 e^{-\beta z} \quad (2.6)$$

Substituting the equation 2.5 and 2.6 in equation 2.3 and 2.4 we get

$$a_0(\beta - \beta_1) - k_{12} b_0 = 0 \quad (2.7)$$

$$b_0 (\beta - \beta_1) - k_{21} a_0 = 0 \quad (2.8)$$

The non trivial solution of equation 2.7 and 2.8

$$B_{s,a} = \frac{(\beta 1 + \beta 2)}{2} \pm \left[\frac{1}{4}(\beta_1 - \beta_2)^2 + k^2\right]^{1/2} \quad (2.9)$$

Thus in coupled waveguide one has two independent set of two modes, one propagating with a propagation constant β_s and the other with β_a. Therefore the general solution of equation 2.3 and 2.4 can be written as

$$A(z) = a_s e^{-\beta s z} + a_a e^{-\beta a z} \quad (2.10)$$

$$B(z) = (\beta_s - \beta_1)\, a_s e^{-\beta s z} / k_{12} + (\beta_a - \beta_1)\, a_s e^{-\beta s z} / k_{12} \qquad 2.11$$

The power in waveguide 1 and 2 is proportional to $|a(z)|^2$ and $|b(z)|^2$. So from equation 2.10 and 2.11

$$|a(z)|^2 = 1 - \frac{4k^2}{\Delta\beta^2 + 4k^2} \sin^2 [(\frac{1}{4} \Delta\beta^2 + k^2)^{1/2} z] \qquad 2.12$$

$$|b(z)|^2 = \frac{4k^2}{\Delta\beta^2 + 4k^2} \sin^2 [(\frac{1}{4} \Delta\beta^2 + k^2)^{1/2} z] \qquad 2.13$$

The coupling length is given by

$$L_c = \pi/2(\frac{1}{4} \Delta\beta^2 + k^2)^{1/2} \qquad 2.14$$

Is called the coupling length of the waveguide coupler and corresponding to the minimum interaction length required for the maximum energy transfer [34]. Complete energy transfer take place when propagation constant in both the waveguide are same for such a case the coupling length becomes

$$L_c = \pi/2k \qquad 2.15$$

This demonstrates one of the nicer features of coupled mode theory. Total power, which is of course given by P1 + P2, is conserved by the device. This is what we would expect, since there is no loss. We can see the variations of P1 and P2 with distance in Fig: 2.4

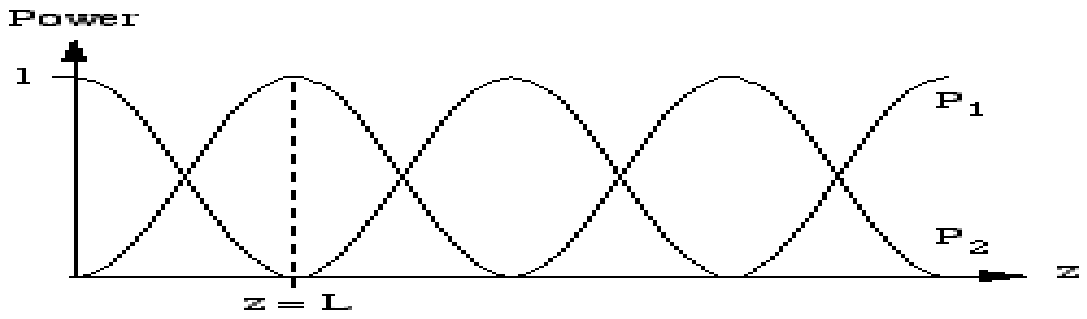

Fig: 2.4 Variation of the powers P1 and P2 with distance z.[33]

As can be seen, the variations are in complete agreement with our earlier qualitative discussion, and the power distribution between the guides is an oscillatory function of z. All the power is transferred from Guide 1 to Guide 2 at the point z = L, when $\kappa L = \pi/2$. Complete transfer also occurs when $\kappa L = 3\pi/2$, $5\pi/2$ and so on.

2.3 Concept of Electro Optic Effect in Waveguide Coupler

Photonic structures that bend, split, couple and filter light have been demonstrated. However such structure have their flow of light predetermined by the design of the structure and cannot be modified once fabricated. There is a high demand to manipulate light beams in waveguide active devices for information processing (e.g. coding – decoding, routing, multiplexing timing, logic operation etc) in high density integrated optic circuit. In previous section we have discuss a waveguide coupler with two identical waveguide. Thus energy incident at the input of one waveguide comes out of the other waveguide at length L_c. if now by some means we can introduce finite $\Delta\beta$ between the two waveguide such that coupling length will change [22]. In order to control the flow of light in waveguide coupler, the refractive index of the waveguide will have to change which in turn change the transmission properties ($\Delta\beta$) [35] of the device. This is the basic principal of active waveguide devices. The propagation constant of two waveguide can be changed through the electro optic effect. Thus by applying the voltage, light can be switch back and forth between the waveguides.

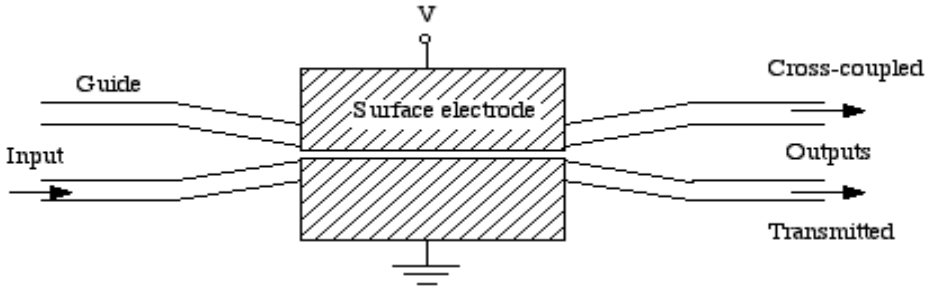

Fig: 2.5: An electro-optic directional coupler switch [19]

if there is a mismatch in propagation constant, so that $\Delta\beta$ is non-zero then the solution of coupled mode equations [22]

$$a(z) = ae^{-i\,\Delta\beta\, z/2} \qquad 2.16$$

$$b(z) = be^{\,i\,\Delta\beta\, z/2} \qquad 2.17$$

we can obtain derivatives of these new variables Substituting into Equations 2.3 and 2.4, we find that all the exponentials cancel out, leaving only constant terms, so that:

$$da/dz - i\Delta\beta/2 + ika = 0 \qquad 2.18$$

$$db/dz - i\Delta\beta/2 + ikb = 0 \qquad 2.19$$

The power output from Guide 2 is given by:

$$|b(z)|^2 = \sin^2[\sqrt{v^2+\zeta^2}]/\ 1+\zeta^2/v^2 \qquad 2.20$$

Where we have introduced two new parameters, a normalised coupling length v and a normalised dephasing parameter ζ, given by:

$$v = k\,L_c \qquad 2.21$$

$$\zeta = \Delta\beta\, L_c/2 \qquad 2.22$$

Equation 2.20 looks a bit like a sinc^2 function (remember that sinc(x) = sin(x) / x). We can plot it out as a function of ξ (together with the power in Guide 1, given by P1 = 1 - P2), for our design value of $v = \pi/2$. This gives the typical switching characteristic shown in Fig: 2.6, 2.7 and 2.8

To make a switch, we therefore need only to be able to define two states:

(i) State A, when no voltage is applied to the device ($\Delta\beta L_c = 0$). The light then emerges from Guide 2.

(ii) State A', when a voltage is applied such that $\Delta\beta L_c = \pi\sqrt{3}$. The light then emerges from Guide 1.

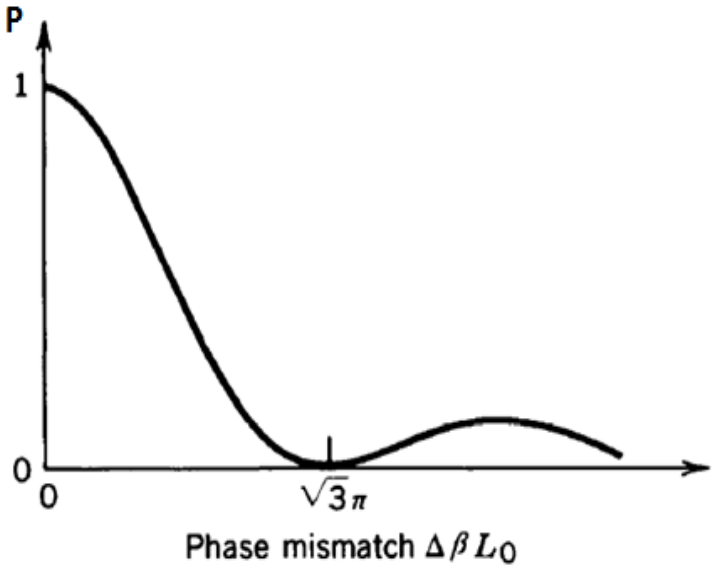

Fig: 2.6 Dependence of power on the phase mismatch. [19]

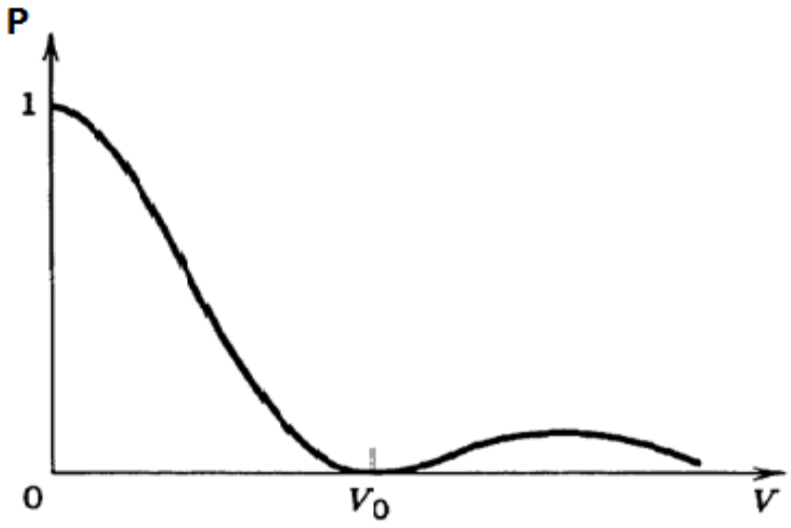

Fig: 2.7 Dependence of the coupling power on the applied voltage V. When V = 0, all of the optical power is coupled from waveguide 1 into waveguide 2; when V =V_0, all of the optical power remains in waveguide 1.[19]

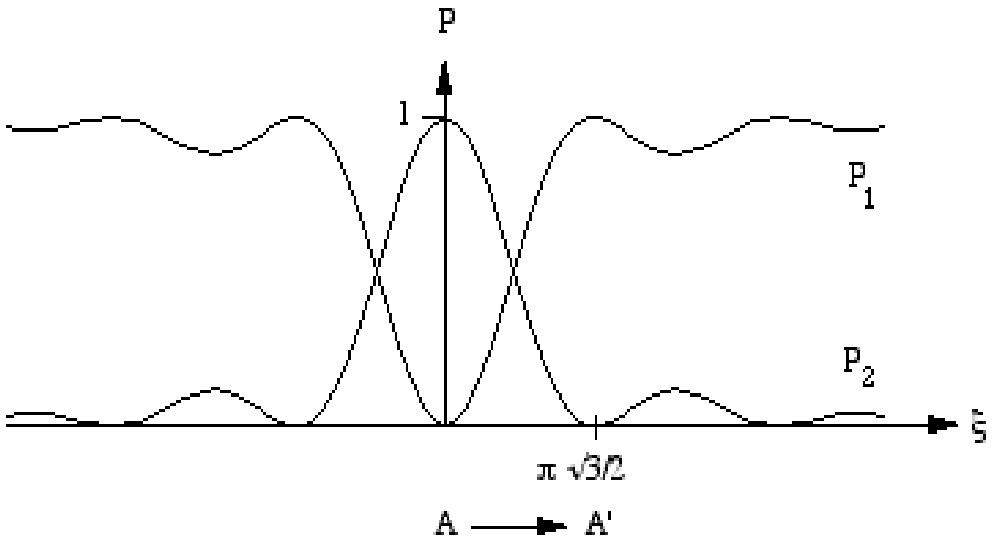

Fig: 2. 8 waveguide coupler switching characteristics [19]

2.4 Different Models of Electro Optic Effect

2.4.1 Pockel and Kerr Effect

The refractive index of an electro-optic medium [14] is a function n(E) of the applied electric field E. This function varies only slightly with E so that it can be expanded in a Taylor's series about E = 0,

$$n(E) = n + a_1 E + 1/2 a_2 E^2 + \quad 2.23$$

Where the coefficients of expansion are n = n(0), $a_1 = (dn/dE)|_{E=0}$, and $a_2 = (d^2n/dE^2)|_{E=0}$. For reasons that will become apparent subsequently, it is conventional to write (2.23) in terms of two new coefficients $r = -2a_1/n^3$ and $s = -a_2/n^3$, known as the electro-optic coefficients, so that

$$n(E) = n - 1/2 r n^3 E - 1/2 s n^3 E^2 + \quad 2.24$$

The second- and higher-order terms of this series are typically many orders of magnitude smaller than n. Terms higher than the third can safely be neglected. The electro-optic coefficients r and s are therefore simply the coefficients of proportionality of the two terms of Δn with E and E^2 respectively.

(a) Pockel Effect

In many materials the third term of Eq. 2.24 is negligible in comparison with the second, where upon

$$n(E) = n - 1/2r\, n^3 E \qquad 2.25$$

Pockels Effect as illustrated in Fig: 2.9(a). The medium is then known as a Pockels medium (or a Pockels cell). The coefficient r is called the Pockels coefficient or the linear electro-optic coefficient; Typical values of r lie in the range 10^{-12} to 10^{-10} m/V (1 to 100 pm/V). For E = 10^6 V/m (10 kV applied across a cell of thickness 1 cm)[11], for example, the term $1/2rn^3E$ in Eq. 2.25 is on the order of 10^{-6} to 10^{-4}. Changes in the effective refractive index induced by electric fields are indeed very small

(b) Kerr Effect

If the material is centrosymmetric, as is the case for gases, liquids, and certain crystals, n(E) must be an even symmetric function [see Fig: 2.9(b)] since it must be invariant to the reversal of E. Its first derivative then vanishes, so that the coefficient r must be zero, whereupon

$$n(E) = n - 1/2sn^3 E^2 \qquad 2.26$$

The material is then known as a Kerr medium (or a Kerr cell). The parameter s is called the Kerr coefficient or the quadratic electro-optic coefficient. Typical values of s are 10^{-18} to10^{-14} m^2/V^2 in crystals and 10^{-22} to 10^{-19} m^2/V^2 in liquids. For E = 10^6 V/m the term$1/2\, sn^3E^2$ in Eq. 2.26 is on the order of 10^{-6} to 10^{-2} in crystals and 10^{-10} to 10^{-7} in liquids.

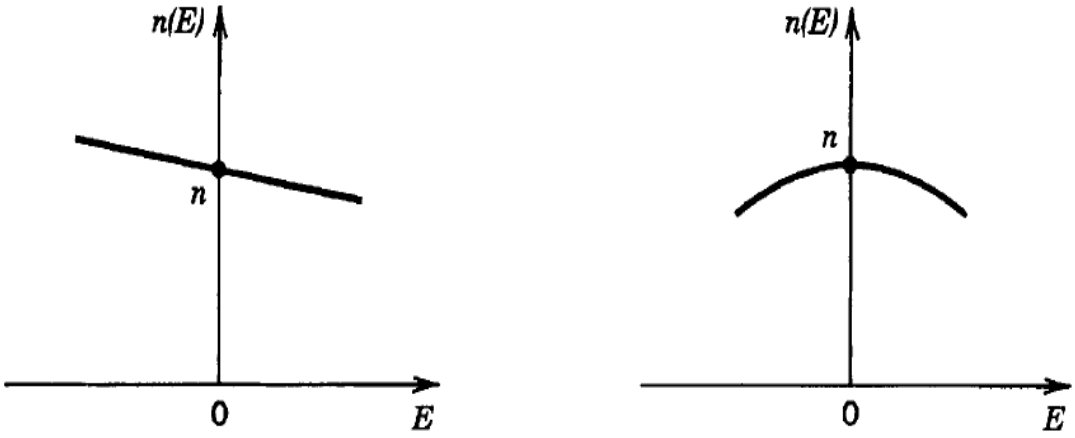

(a) **(b)**

Fig: 2.9 Dependence of the refractive index on the electric field: (a) Pockels medium (b) Kerr medium [14].

2.4.2 Franz Keldysh Effect

A significant contribution to the quadratic electro-optic effect in InP and InGaAsP is the Franz-Keldysh effect. It was proposed independently at the same time by W. Franz and L.V. Keldysh in 1958 [36]. The Franz Keldysh effect is an electric field induced photon assisted tunnelling effect. By lowering the effective band-gap energy in a crystal in the presence of an electric field, it acts on the absorption index and on the refractive index. The physics of the Franz Keldysh effect can be explained by band deformation in the presence of electric fields. Normally a semiconductor crystal is transparent for photon energies below the bandgap energy. In the presence of an electric field, as it occurs in a p-n junction, however, the conduction and valence band are bent. The bending of energy bands makes tunnelling from the valence to the conduction band possible (see Fig: 2.10). The electrons have to tunnel through a triangular barrier, that is the smaller the photon energy is to the bandgap energy and the higher the electric field is, because the tunnelling distance Δx; decreases with increasing electric field. Thus the tunnelling probability, and thereby the absorption index, increases with the higher electric fields and photon energies. Since the initial calculations of W. Franz and L. Keldysh a detailed theoretical study of the electric field dependency of the optical absorption near normal absorption edges has

been carried out for direct and indirect transitions. Some experimental verification of these theoretical works has been done either by direct absorption measurements or reflection measurements.

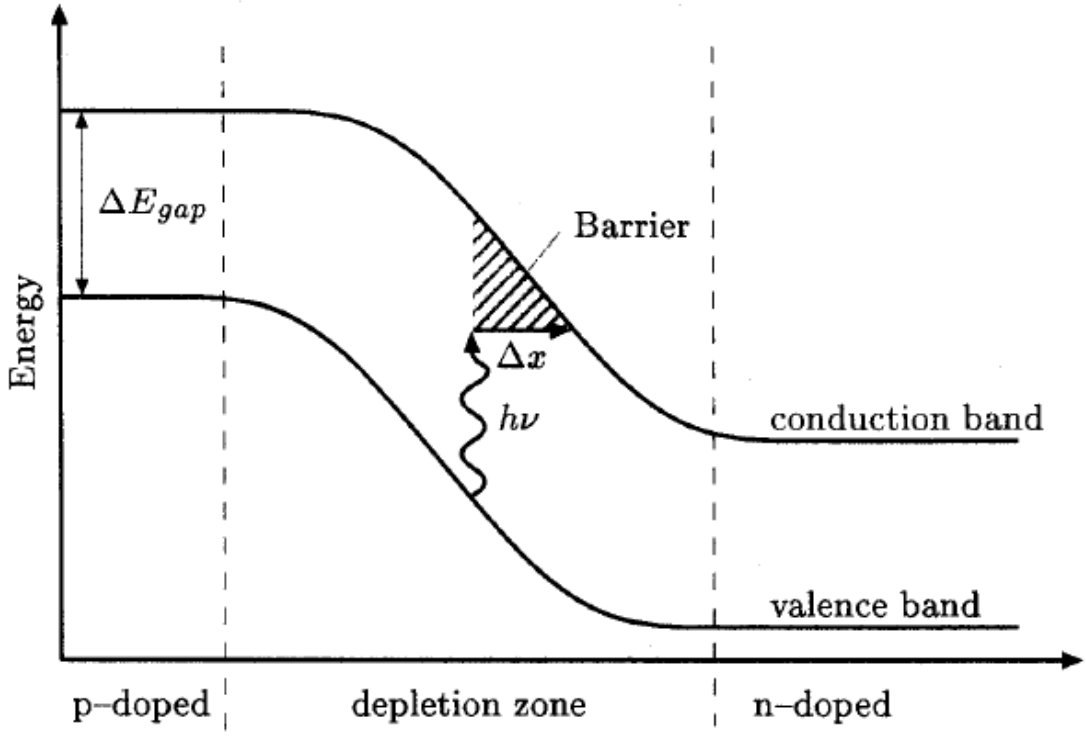

Fig: 2.10 Photon assisted tunnelling of an electron in Franz Keldysh effect [36]

2.4.3 Carrier Plasma Dispersion Effect

The plasma dispersion effect (also known as charge carrier effect) arises because the optical properties of material are affected by introducing free carrier into an undoped sample [37, 38].The relationship between a change in the refractive index and a change in optical absorption due to change in free carrier concentration is given by [39]

$$\Delta n = \left\{\frac{e^2\lambda^2}{8\pi^2 c^2 \varepsilon_0 n}\right\}\left[\frac{\Delta N}{m_{ce}} + \frac{\Delta P}{m_{ch}}\right] \quad 2.27$$

$$\Delta \alpha = \left\{\frac{e^2\lambda^2}{8\pi^2 c^3 \varepsilon_0 n}\right\}\left[\frac{\Delta N}{m_{ce}^2 \mu_e} + \frac{\Delta P}{m_{ch}^2 \mu_h}\right] \quad 2.28$$

Where e is the electron charge ,ε_0 is the permittivity , n is the unperturbed refractive index, m_{ce} is the conductivity effective mass of electron , m_{ch} is the conductivity

effective mass of hole, μ_e is the electron mobility and μ_h is the hole mobility. Simplified equation

$$\Delta n = \Delta n_e + \Delta n_h$$

$$= - [8.8 \text{ X } 10^{-22} \Delta N + 8.5 \text{ X } 10^{-18} (\Delta P)^{0.8}] \quad 2.29$$

$$\Delta \alpha = \Delta \alpha_e + \Delta \alpha_h$$

$$= 8.5 X 10^{-18} \Delta N + 6.0 X 10^{-18} \Delta P \quad 2.30$$

Where Δn_e is the refractive index change due to the electron concentration change, Δn_h is the refractive index change due to hole concentration change, $\Delta N(cm^{-3})$ is the electron concentration change, $\Delta P(cm^{-3})$ is the hole concentration change, $\Delta \alpha_e$ $(cm^{-1})$is the absorption coefficient variation due to ΔN, $\Delta \alpha_h$ (cm^{-1}) is the absorption coefficient variation due to ΔP

2.5 Silicon on Insulator (SOI): An Integrated Platform for Silicon Photonics

Silicon-on-insulator (SOI) circuits [13] are composed of three components; an insulating layer (Silicon dioxide, Sapphire, etc.) on the bottom, a crystalline Silicon layer above it and a final cladding layer on top. The cladding layer can be Silicon oxide, air or any other material with a low refractive index. The high difference in index of refraction (n) between Silicon (~3.5), Silicon dioxide (~1.44) and Air (1.00) allows for optimal transmission of electromagnetic waves.

Another reason for the use of SOI chips is that silicon fabrication techniques (CMOS) have become increasingly refined over the past couple decades, motivated by increasing computer power and efficiency. Currently, SOI technology [17] is in its infancy and is being explored as an alternative to electrical circuits in a variety of applications. It may begin to replace CMOS technology once the fabrication cost decreases. However, it is still the predominate process used in the fabrication of Silicon photonics.

In Silicon photonics, the sandwiched crystalline silicon layer is used to fabricate optical waveguides in addition to other passive optical devices such as racetrack resonators or

more generally, optical multiplexers and demultiplexers. Because of the aforementioned differences in the index of refraction, and the fact that Silicon is transparent to infrared light with wavelengths above 1100nm, electromagnetic waves are able to propagate in the waveguides on the basis of total internal reflection.

In this section the structure of an SOI wafer and waveguide structures are exposed. Various materials such as silicon, InP, and SiO2 have been used to implement optical waveguide coupler devices. Recently, silicon-on-insulator (SOI) has emerged as highly promising due to its excellent optical properties and the compatibility with the well developed CMOS integrated circuit technology. Besides, the size of the photonic components based on SOI could be reduced dramatically compared to the one based on SiO2 due to the high refractive index contrast between silicon (n = 3.44) and SiO2 (n = 1.46). For the SOI waveguide [40], a rib waveguide (Fig: 2.11) is preferred since it could give a high coupling efficiency to a standard single mode fiber. The configuration of an SOI wafer is shown in Fig: 2.12. A silicon dioxide layer is grown under the surface of the silicon wafer. The top layer is then used as the guiding layer.

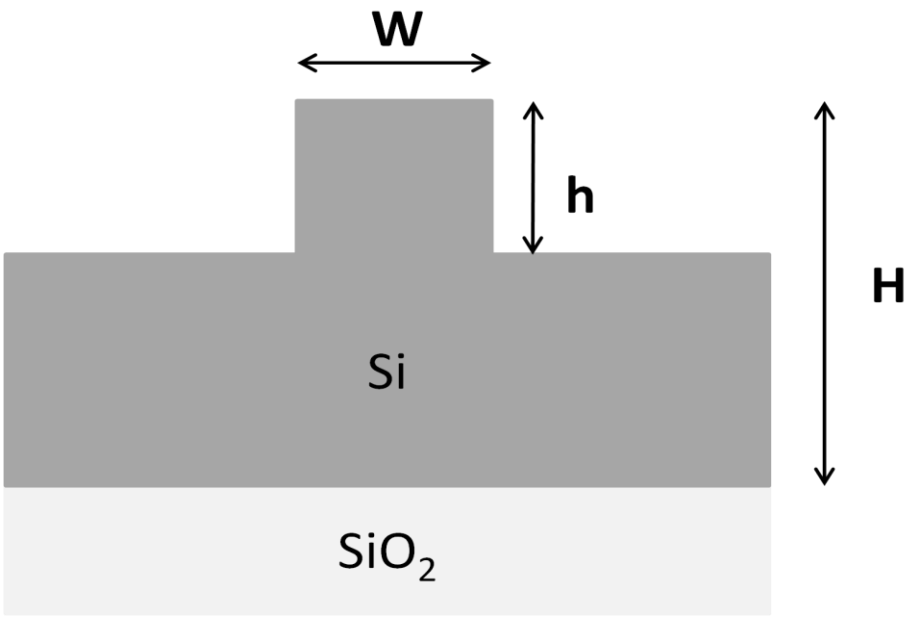

Fig. 2.11 Rib waveguide cross section

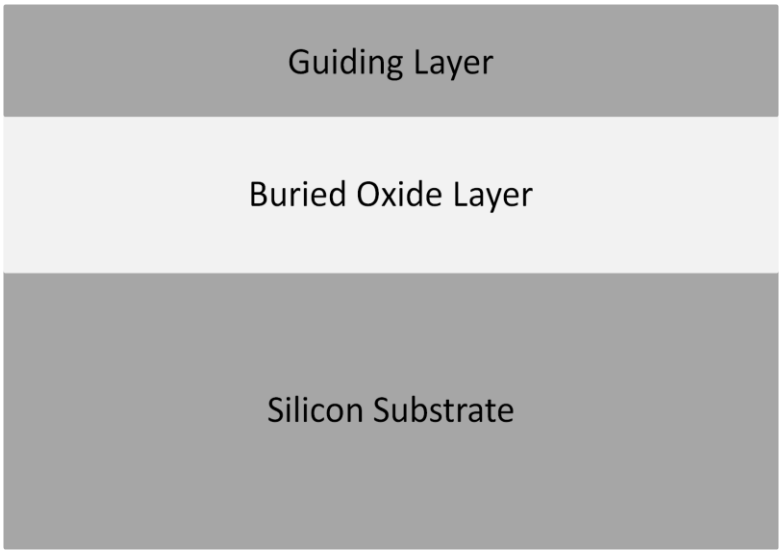

Fig: 2.12 SOI wafer structure

.2.5.1 SOI Waveguide Coupler

SOI chips are being considered as a viable alternative for transmitting high bandwidth data over medium distances currently dominated by more conventional technology. The current technology relies on data being transmitted along metal wires via electrical pulses. The SOI chips are capable of transmitting light pulses and are therefore capable of much higher bandwidth signals with much less noise[39, 41].

Silicon-on-insulator (SOI) optical waveguides have emerged as an attractive class of optical waveguide elements recently [42]. The SOI technique possesses good characteristics such as low leakage current and high optical light confinement for researchers to design advanced low-power, high-speed opto-electronic devices. In addition, the electro optic effect has also been demonstrated in Si waveguides for the manuplating the light beam. This give the motivation is to design a SOI configuration that will act as a waveguide coupler, i.e. to design a device that that will couple the power between the waveguides at different applied voltage across the device. The characteristics of this electro-optic waveguide coupler will determine the minimum coupling length between the waveguide at different applied voltage.

Chapter 3

Literature survey

Today's evolving telecommunication networks are increasingly focusing on flexibility and reconfigurability, which requires enhanced functionality of photonic integrated circuits (PICs) [20] for optical communications. The birth of optical communication coincided with the fabrication of high speed active waveguide devices [11]. Ever since, the scientific and technological progress in this field has been so phenomenal that we are already in the fifth generation of optical fiber communication systems. Recent developments in optical amplifiers and wavelength division multiplexing (WDM) are taking us to a communication system with almost "zero" loss and "infinite" bandwidth. For this, Morden wavelength division multiplexing (WDM) systems require signal routing and coupling devices to have large optical bandwidth .Optical waveguide coupler has emerged as powerful analysis tool with vast applications in optical telecommunication systems.

Optical waveguides [26] are key components in integrated photonic guided wave devices. The concept of guided wave devices was first given by John Tyndall (1820-1893), 19th century physicist, when he observed that that a jet of water can act to confine light. The first waveguide was proposed by J. J. Thomson in 1893 and experimentally verified by Oliver Lodge in 1894; the mathematical analysis of the propagating modes within a hollow metal cylinder was first performed by Lord Rayleigh in 1897. Which lead to the concept of mode coupling between the waveguides [31].

The concept of coupled modes [32] in electromagnetics may be traced back to the early 1950's. The application was initially to microwaves and developed gradually through the contributions of many people. In 1954, Pierce applied the coupled mode theory to the analysis of microwave travelling-wave tubes. Later followed the work of Gould on the backward-wave oscillators, the coupled mode theory was then employed to treat parametric amplifiers, oscillators, and frequency converters. A parallel development happened in microwave waveguides and devices [3]. Miller first introduced the coupled mode theory to the analysis and design of microwave waveguides and passive devices.

The theory was soon generalized by Louisell to treat tapered waveguide structures, where the coupling coefficients depend on the length *z*.

In the 1960's, the coupled mode theory was further developed to describe mode conversions due to various irregularities in microwave waveguides and periodic waveguide structures. The coupled mode theory for optical waveguides [33] was developed by Marcuse, Snyder Yariv and Taylor, and Kogelnik in the early 1970's. It has been successfully applied to the modelling and analysis of various guided-wave optoelectronic and fiber optical devices, such as optical directional couplers made of thin film and channel waveguides and optical fibers ,multiple waveguide lenses ,phase-locked laser arrays , distributed feedback lasers and distributed Bragg reflectors ,grating waveguides and couplers .

Luckosz and Tiefenthaler reported evanescent field tuning in planar optical waveguides [43] in 1983. The authors discovered variations in the effective index of the guided modes of high refractive index waveguides upon changes in their environment, e.g. ambient humidity. Evanescent field tuning is now well established and used extensively in planar light wave circuits. Some examples of optical evanescent field devices in the literature include Mach–Zehnder interferometer, channel waveguide, directional coupler, and multi-mode interference couplers. In order to control transmission properties in active waveguide devices raises a fundamental problem of manipulating the light beam for information processing in high density integrated optic circuits. The main methods to change the transmission properties of active waveguide devices are thermo-optic effect [15] and electro-optic effect. The electro optic effect was first discovered by John Kerr and Friedrich Pockel in 1875 and 1893 respectively in electro optic material [14]. While, in January 1990 Brainr R. Bennett, Richard A. Soref, and Jesus A. Delalamo have theoretically estimated the change in transmission properties of material by injection of free carriers in InP, GaAs and InGaAsP employed free-carrier plasma effect. Refractive index changes as large as 10^{-2} are predicted for carrier concentrations of $10^{18}/cm^3$ [38, 39], suggesting that low-loss optical phase modulators and switches using carrier injection are feasible in these materials.

Research methodologies developed within the last decade in the field of active waveguide couplers (switches and modulators) are presented below.

Design of an integrated electro-optic switch in organic polymers [44] was first presented by P. Kaczmarski, J..P.Vande Capelle, P.E.Lagasse and R.Meynart 1989. The proposed design is tunable in both switching state. The optimized parameter of the proposed design show the polarization voltage of 10 volt in both the state and switching length is equal to 1mm.

Wei Yu Lee, Jin Shin Lin, and Sung Yuen Wang in 1995 have presented a novel Δk directional coupler switch using liquid crystal (LC) [45]. For decreasing the switching length of the directional coupler switch, the electro-optic properties of LC is used and calculated results present the relevant design considerations of the switch. Because of the large birefringence of LC's, a very short switching length of *60 μm* is reported.

Optical multi mode interference device based on self imaging principal [46] were presented first by Lucas B. Soldano and Erik C. M. Pennings, in April 1995 which gives an overview of integrated optics routing and coupling devices based on multi mode interference. The underlying self imaging principal in multimode waveguide described using a guided mode propagation analysis. Special issues concerning the design and operation of multimode interference devices are discussed and 235 *μm* coupling length has been optimized.

In 2003 R. Chakraborty, J.C. Biswas, S.K. Lahiri have analyzed the electro-optic switch using Effective index based matrix method [47]. The analysis is focused on directional coupler switching devices made by $LiNbO_3$ and characteristics are derived from the distributions of optical power and electrical modulating field within the device. By optimising the structure, coupling length of 1954.3μm are observed with the application of 19 volt across the device

Electro optic modulation of SOI waveguide devices [48] have been proposed by C. Angulo Barrios, V. R. Almeida and M. Lipson, in 2003. The electro optic structure is electrically and optically modelled. The effect of the waveguide geometry on the device performance is studied with lateral definition of PIN diode.

Hybrid Silicon/ Electro-optic Polymer Modulator was modelled by Kjersti Kleven and Scott T. Dunham in 2005. The device incorporates a hybrid silicon/electro-optic polymer waveguide [49] in the cavity region with a distributed Bragg reflector in a single mode silicon waveguide on each side of the cavity to create a modulator with a large modulation depth, short device length and a low drive voltage for use in future high speed integrated optics applications. The total active device length for this modulator is observed only 28 μm with 91% of modulation depth

Fan Wang, Jianyi Yang presented an optical switch based on MMI in 2006. MMI is demonstrated in this switch [50]. The device is designed and fabricated in polymeric materials and the thermo optic (TO) effect of polymers, which has a negative TO coefficient [51], is employed to change the self-imaging effect of a side-heated MMI coupler and realize optical switching. The experimental result shows that power is switched in cross and bar state with the device length of about 3.3*mm*.

Recent advances in high speed silicon optical modulator [52] were presented by Ansheng Liu, Ling Liao, Doron Rubin, and Hat Nguyen in 2007. High-speed silicon optical modulator is one of key components for integrated silicon photonic chip aiming at *Tb/s* data transmission for next generation communication networks as well as future high performance computing applications. In particular, high-speed and highly scalable silicon optical modulator based on the free carrier plasma dispersion effect is presented in this research proposal

Simulation and optimization of a polymer directional coupler electro-optic switch with push–pull electrodes [53] is demonstrated by Chuan-Tao Zheng, Chun-Sheng Ma, Xin Yan, Xian-Yin Wang, Da-Ming Zhang in 2008. Structural model and design technique are proposed for a polymer directional coupler electro-optic switch with rib waveguides and push–pull electrodes, of which the electric field distribution is analyzed by the conformal transforming method and image method. In order to get the minimum mode loss and the minimum switching voltage, the parameters of the waveguide and electrode are optimized, such as the core with, core thickness, buffer layer between the core and the electrode, coupling gap between the waveguides, electrode thickness, electrode width and

electrode gap. Coupling length of $3082\mu m$ is reported with the application of 2.14 volt across the device

In 2009, design of ultra fast polymer electro-optic waveguide switch [54] for Intelligent Optical Networks was presented by S.Ponmalar, S.Sundaravadivelu. The performances of the 2x2 optical waveguide switch with rectangular, triangular and trapezoidal grating profiles on various device parameters were analyzed. The simulation result shows that trapezoidal grating is the optimized structure which has the coupling length of 81μm and switching voltage of 11V for the operating wavelength of 1550nm.

Ravi J. McCosker and Graham E. Town described and analyzed the phenomenon of partial image revivals in a multi-channel directional-coupler (MCDC) structure [55] in 2010. Using supermodes, a MCDC is described as a composite waveguide structure and then analyzed in terms of multi-mode interference and the principle of self-imaging.

P. Dong, Shirong Liao, Hong Liang, Roshanak Shafiiha, Dazeng Feng, Guoliang presented submilliwatt, ultrafast and broadband electro-optic silicon switches in 2010. Forward-biased p-i-n junctions are employed to tune the phase of silicon waveguides in the MZI, to achieve a π-phase switching power of 0.6 *mW* with a drive voltage 0.83 V with a MZI arm length of 4 *mm* [56].

Delta-k electro-optic modulator for 1310 *nm* using a multi-channel directional coupler structure has been described by R. J. McCosker _ G. E. Town in 2011. The device employed a poled electro-optic polymer material for the cladding layer [57]. Using an electrode thickness of 2 *mm* and a top drive electrode width of 12 *mm* the device is both velocity and impedance matched to 50 *Ω*. Numerical simulations for a device length of 5.25 *mm* demonstrate a 3-*dB* modulation band- width of 176 *GHz* and a drive voltage of 16.5 V.

Higher modulation efficiency in electro optic polymer modulator with slotted silicon waveguide is achieved in 2011 Silicon slot waveguide based Mach–Zehnder interferometric modulators with electro optic polymers in the slot have the advantage of low half-wave voltage-length product Surface passivation of silicon nanophotonic structures [58] has been found to be effective in improving poling efficiency. By applying these techniques to a silicon slot waveguide Mach–Zehnder modulator, a low V *L of 0.52 V cm has been achieved.

In 2012 A numerical investigation, based on the use of split step Fourier transformation algorithm, of all-optical solitons switching in asymmetric directional couplers [59] is presented by Qiliang Li, Aixin Zhang, Xiaofeng Hua The analysis highlights the influence of the different effective mode area, the phase- and group–velocity mismatch, the different dispersion between two cores on the switching and propagation of short pulses. The investigation indicates that the phase velocity mismatch and the different effective mode area can reduce the coupling length while the different group velocity and the different dispersion between two cores do not change the coupling length

Kenjal jain and Prof. H.K.Dixit presented the concept of optimize of 2x2 Mach-Zehnder interferometer electro-optic switch [60] in 2012. The optimization of switching characteristics is performed for low switching losses such as insertion loss, excess loss, high extinction ratio and low switching voltage by varying the gap of 3*dB* couplers, gap of interferometric arms and waveguide width. Further observation has been made by changing waveguide width the switching voltage is reduced from 7.8 V to 7.4 V.

Integrated multimode interference coupler-based Mach–Zehnder interferometric modulator [61] fabricated on a silicon-on-insulator substrate has been presented by R.W. Chuang, M.T. Hsu, Y.C.Chang Y.J. Lee and S.H.Chou in 2012. The design of the device have 6000x40μm Mach–Zehnder interferometric (MZI) electro-optic modulator fabricated on silicon-on-insulator (SOI) substrate based on a back-to-back cascade of two 1 × 2 multimode interference (MMI) couplers for the operating wavelength of 1.55 *mm*. A signal modulation is achieved with the incorporation of a phase shifter in one of the two arms that connect two MMI devices together and the resultant extinction ratio achieved is in the excess of -25 *dB*.

Ultra-compact high-speed electro-optic switch utilizing hybrid metal-silicon waveguides has been proposed by Eric F. Dudley and Wounjhang Park in 2013. They described the basic properties of such waveguides, discussed the behaviour of hybrid waveguide directional couplers [62] and presented a design for an ultra-compact electro-optic switch based on these properties. At 1 V drive voltage, switching at speeds up to 30 *Gbits/sec* can be achieved in a device that is 30 μm long.

In 2013 Shiyang Zhu, G. Q. Lo, and D. L. Kwong presented ultracompact si electro-optic modulator based on horizontal Cu-insulator-Si-insulator-Cu nanoplasmonic waveguide on SOI substrates using standard CMOS technology [63]. A modulator with 1µm long phase shifter exhibits 9-dB extinction ratio under 6-V/10-*kHz* voltage swing.

Chapter 4

Design and simulation of electronically tunable SOI waveguide coupler

4.1 Introduction

In chapter 2, the theory of optical waveguide coupler, various electro-optic effect and basics of SOI waveguide structure were discussed. A variety of waveguide devices including electro-optic switch, tunable [64] wavelength demultiplexer/ multiplexer and electro-optic phase modulator can be developed by controlling the guided waves that are confined in waveguides with external input signals. The guided waves are controlled via electro-optic. Most of the waveguide couplers are made up of lithium niobate ($LiNbO_3$) and polymer. Utilising of electro–optic effect in these material posses difficulties because of small change in refractive index (Δn) at high voltage and higher power consumption, along with rather long coupling length. Intrinsic bandwidth limitation of 40 *GHz* has been reported for $LiNbO_3$ and at the same time polymer suffers from thermal, molecular orientation and photochemical instabilities that can result in device degradation. All of these conditions are undesirable in practical systems. Therefore the use of polymer and $LiNbO_3$ become the major issue in designing of waveguide coupler for high speed operation and low power consumption.

The use of silicon for optical waveguide coupler would enable a platform for a monolithic integration of optics and microelectronics. In order to control the flow of light in Si waveguide coupler, active devices (modulator and switch) need to be developed in silicon, where change in the effective refractive index induces a change in the transmission properties of the devices [39].

The main methods to alter the effective index in Si are the thermo optic effect and electro–optic effect. The thermal change of optical refractive index in Si is large. However the thermo-optic effect is rather slow and can be used only up to 1 MHz modulation frequencies. For higher modulation frequencies, up to a few hundreds of

mega hertz electro–optic devices are required. One of the main challenges of using silicon as an active photonics material is its low electro optic coefficient. The most common electro–optic effect found in compound semiconductor is weak in silicon. Unstrained pure crystalline silicon does not exhibit a linear electro–optic (Pockel) effect. The Franz Keldysh effect and the Kerr effect ("the second order electro optic effect") have very low efficiencies. A refractive index variation of $\Delta n \sim 10^{-5}$ in the near infrared for the Franz Keldysh effect and $\Delta n \sim 10^{-8}$ for the Kerr effect for an applied field of 10^5 V/Cm. Therefore high electromagnetic fields potentially close to the breakdown of silicon are required in order to achieve a useful change in the index of refraction (Δn).

The most effective mechanism for changing the effective refractive index in Si at a fast rate is the carrier plasma dispersion effect, which also has the advantage of being polarization independent. The free carrier concentration in electro–optic devices can be varied by injection, accumulation, depletion or inversion of carrier. PIN diode may be employed for this purpose. In PIN configuration carrier can be injected in a large area (intrinsic region) in order to maximize the aforementioned overlap, increasing the effective index change.

In this work, A electro optic waveguide coupler based on carrier plasma dispersion effect utilising silicon on insulator sub micrometer size rib waveguides structure has been introduced, then we describe the phenomenon of partial image revivals and complete image revivals, in order to reduce the coupling length in a waveguide coupler structure and analyzed in terms of multi-mode interference and the principle of self-imaging [46]. Reduction in coupling length of waveguide coupler for active waveguide devices has been a challenging subject. To achieve this objective, the structures of waveguide coupler for min coupling length are designed and simulated.

4.2 Principal of Self Imaging

Coupled-mode theory (CMT)[32] has been successfully employed to analyze multi-waveguide structures .The accuracy of CMT is dependent on a weak coupling regime , that is, the individual waveguides are weakly perturbed by the close proximity of the other guides. Various authors have used CMT based on the classification of eigen-values

to analyze so-called waveguide arrays in terms of the evolution of the amplitude of the optical field of each waveguide.

In this work, we describe a waveguide coupler as a single composite waveguide structure that supports multi-modes or supermodes , as shown in Figure:4.1. The operation of the MCDC can then be analyzed in terms of multi-mode interference (MMI) for periodic self-imaging principal. In other words, each supermode propagates with a different phase velocity and hence forms an interference pattern along the device, and as a result, image revivals of the input field form at periodic intervals along the direction of propagation.

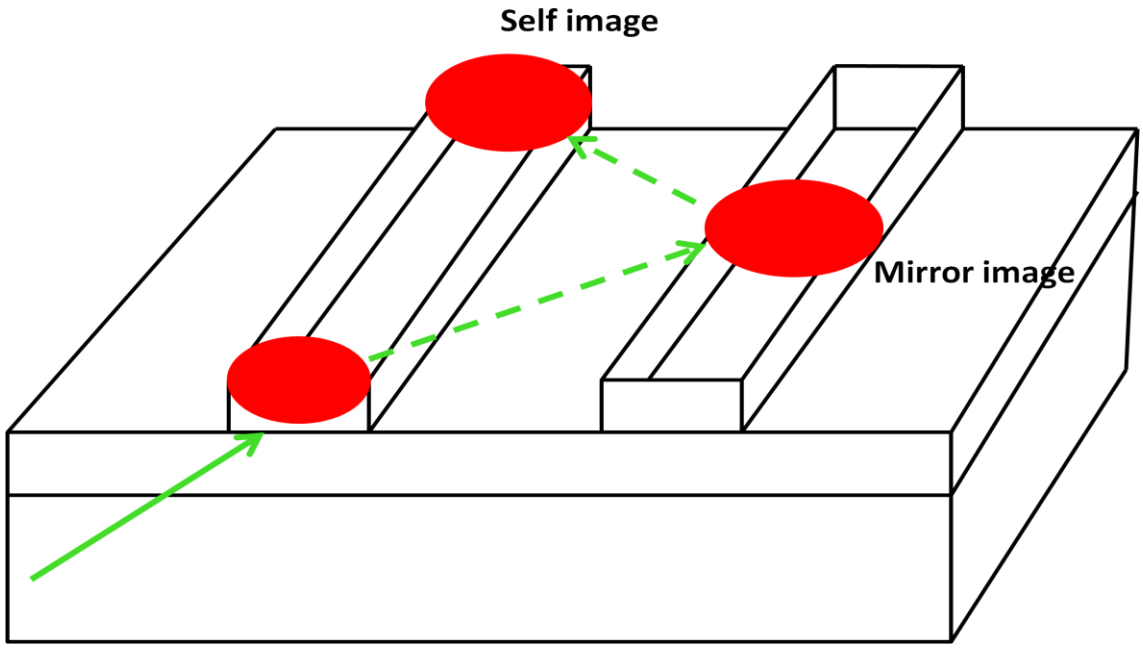

Fig: 4.1 Scheamatic of waveguide coupler, the imaging points that evolve along the direction of propagation of the device are shown

Consider a waveguide coupler that consists of two identical channel waveguides of width w separated by a distance g, as shown in fig: 5.4. The two waveguides are in such close proximity that the evanescent fields that extend into the space between the waveguides, interact. The coupling between two symmetric waveguides can be approximated by[65,66]

$$k = 2\sqrt{n_c^2 - n_a^2}\,\frac{k}{\beta w_{eff}}\exp\left\{-\sqrt{\beta^2 - (n_a k)^2}\left(s + \frac{w}{2}\right)\right\} \qquad 4.1$$

Where n_c denotes the waveguide core refractive index; n_a denotes the analyte refractive index; β denotes the unperturbed propagation constant common to each waveguide;

Multimode

Consider a 2-channel waveguide coupler, which consists of two identical channel waveguides, as shown in Fig: 4.1. For the following analysis, uniform coupling between the waveguides is assumed, that is, $k = k_{12} = k_{21}$

which denotes the coupling coefficient between waveguides 1 and 2; . The electric field distribution of the device can be viewed as the superposition of the decoupled waveguide modes [55]

$$E(x,y,z,t) = \Sigma_{n=1}^{2} A_n(z)\, E_n(x,y) \exp[j(\omega t - \beta z)] \quad 4.2$$

Where $A_n(z)$ denote the perturbed mode amplitudes as a result of coupling; β denotes the propagation constant common to each identical decoupled waveguide, and $E_n(x\ y)$ denote their guided mode profiles. The time dependent term exp ($j\omega t$) is assumed implicit hereafter. The new mode amplitudes can be defined as

$$a_i(z) = A_i(z) \exp(-j\beta z) \quad 4.3$$

And obey the coupled mode

$$j\frac{da}{dz} = Ma \quad 4.4$$

The matrix M is defined as

$$\begin{bmatrix} \beta & k \\ k & \beta \end{bmatrix} \quad 4.5$$

The array coupling coefficients k are constant, which means they are independent of the propagation direction *z*, and therefore we can assume the mode amplitudes evolve as

$$a_v(z) = a_v(0)\exp(-j\sigma_v z) \qquad v = 1,2 \qquad 4.6$$

Corresponding supermode propagation constants are given by

$\sigma_1 = \beta - k$

$\sigma_2 = \beta + k$

Propagation Analysis

The supermode profiles are defined as

$$E_v(x) = \Sigma_{n=1}^{2} a_v(0)\, E_n(x) \qquad 4.7$$

The field profile for a 2-channel Waveguide coupler at a distance z can be written as a superposition of all the supermode field distributions

$$E(x,y,z) = \Sigma_{n=1}^{2} E_v(x)\exp(-j\sigma_v z) \qquad 4.8$$

For a waveguide coupler, the two supermodes propagation is shown in Fig:4.1 . If we assume the phase of the fundamental supermode σ as a common factor then Eq.4.7 can be rewritten in terms of the supermode propagation constants spacing by

$$E(x,y,z) = \Sigma_{n=1}^{2} E_v(x)\exp[-j(\sigma_1 - \sigma_2)z] \qquad 4.9$$

Taking into account the symmetry stated, an inspection of Eq.4.9 shows that the field distribution at a distance z = L will be a mirror-image of the input field if

$$\exp[-j(\sigma_1 - \sigma_2)L] = (-1)^v$$

In this case, the phase changes must be alternately even and odd multiples of π, which means the even modes are inphase and the odd modes are in anti-phase. Alternatively, an inspection of Eq.4.9 shows that the field distribution at a distance z = L will be a self-image of the input field if

$\exp[-j(\sigma_1 - \sigma_2)L] = 1$

4.2.1 Complete Image Revivals

The supermodes beat along the direction of propagation to form periodic mirror- and self-images of the input field as discuss above, The Fig: 4.2 show the power evolution for a waveguide coupler, which illustrates a consistent periodic mirror- and self-image phenomenon. Furthermore, this figure indicates that the mirror- and self-images are complete image revivals of the input field. That is, a mirror-image corresponds to the input field being completely revived on the opposite side or output (top) waveguide. Whereas, a self-image corresponds to the field being completed revived on the input (bottom) waveguide The self-image length for a waveguide coupler coupler is given by

$$L = \frac{i\pi}{\sigma_1 - \sigma_2} \qquad 5.10$$

Which corresponds to a 2π phase difference between the supermodes, and is twice that of the mirror-image length. Where the parity of i denotes whether the image formed is either a mirror-image (odd) or a self-image (even).

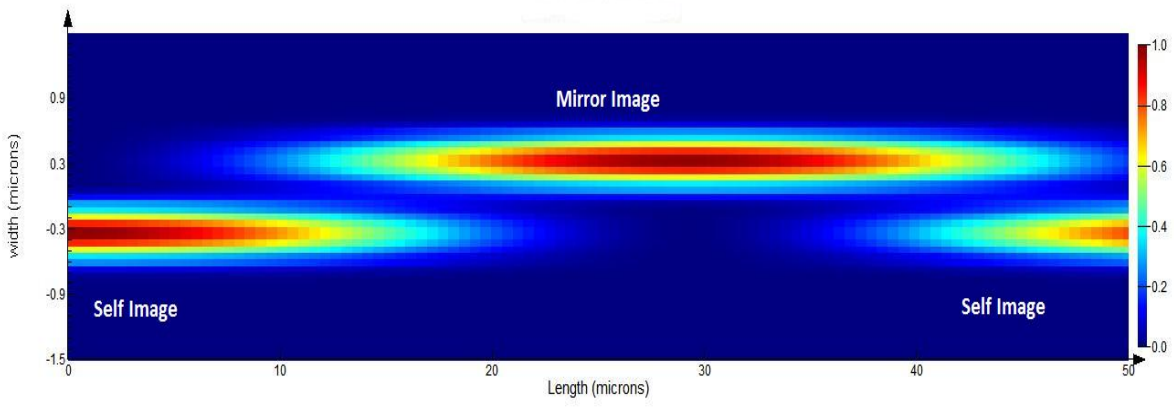

Fig: 4.2 Simulated power evolution along a 2-channel waveguide coupler that shows consistent periodic mirror- and self imaging phenomenon

4.2.2 Partial Image Revivals

In the case of stronger coupling, high-order beating between the supermodes starts to have an influence within the mirror- and self-image range. This results in the replacement of the periodic complete images with a series of partial image revivals.

If we bring the waveguides in the array closer together we increase the coupling between the waveguides themselves. The increased coupling results in a quicker transfer of energy between the waveguides, and according to Eq.4.1 results in shorter mirror- and self-image lengths. However, as the waveguides get close enough together, the power evolution of the waveguide coupler begins to exhibit a more complex interference pattern between the supermodes. The result is the formation of what we refer to as partial image revivals at periodic intervals along the direction of propagation. The simulated power evolution is shown in Fig: 4.3, which shows partial image revivals.

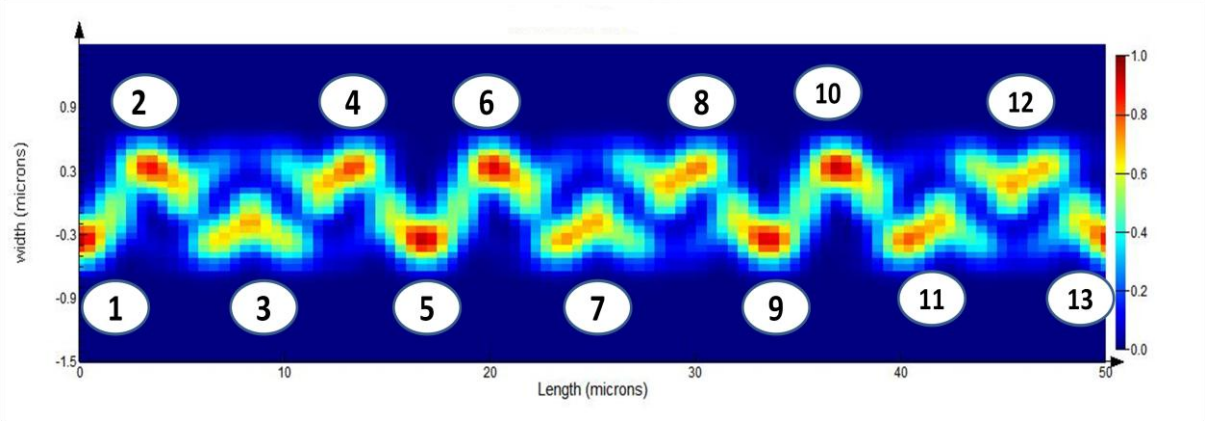

Fig: 4.3 Simulated power evolution along a waveguide coupler that shows partial imag--ing phenomenon; with Partial mirror-images: 2, 4, 6, 8, 10 and 12; Partial self Image:1, 3, 5, 7,9,11 and 13.

4.3 Proposed Design of Electronically Tunable SOI Waveguide Coupler

We have proposed the design of the electronically tunable SOI waveguide coupler based on the free carrier plasma effect. The design of the device is based on that of a p-i-n

diode. The waveguide couplers are fabricated using silicon-on-insulator (SOI) wafers with a 0.11-μm-thick layer of silicon above a 3.89-μm buried oxide. The device employed SOI rib waveguide structure with rib height of h. The coupler has an input and add/drop waveguide width w μm and gap between the waveguide is g. . For tuning in coupling length forward bias PIN configuration is used. Thus the intrinsic region includes 400nm+2w μm +g of slab region and 2w μm of rib waveguides. It consists of a high-aspect-ratio [rib height> slab height] rib SOI waveguide with a p^+ region and an n^+ region defined in the slab, which are 200nm away from the edge of the rib. The p^+ and n^+ regions of silicon layer (device layer) has an a uniform doping concentration of 10^{18} cm^{-3}. To make electrical contact to the core of the waveguide, 1.4 μm region of silicon slab under the metal contacts on both side heavily doped, (n^{++} and p^{++}) with doping concentration of 10^{19} $cm-3$ in order to ensure good ohmic contact .the waveguides is connected to metal contacts located 3 μm away from the edge of ribs.

•

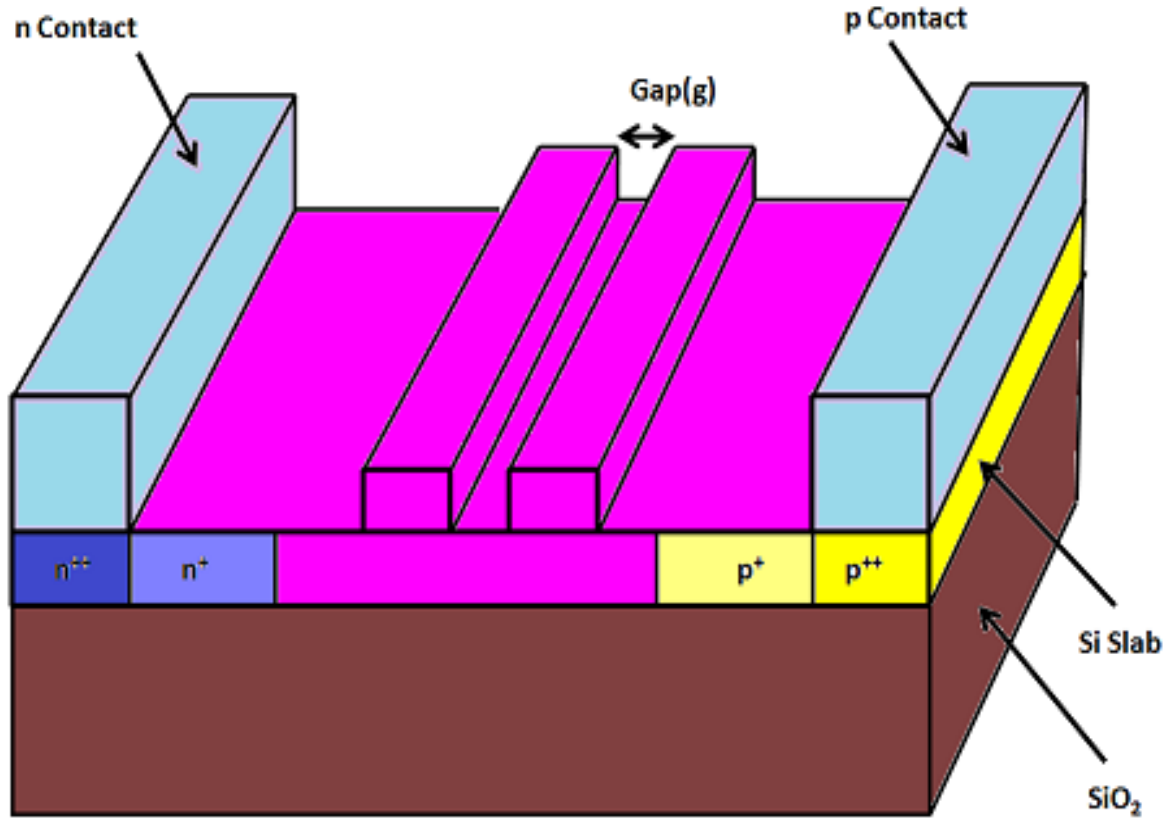

Fig: 4.4 Schematic of the proposed waveguide coupler. Waveguide parameter – height h, width w and gap g

4.4 Simulation Results and Discussion

In wave guide coupler when a beam of light is launched into guide 1 power gets coupled to guide 2 after traversing the switching length of L_c. However fraction of power gets coupled will be a strong function of gap between the waveguide and waveguide geometry. Therefore we use this as a starting point and do a further numerical optimization of the structure. We will now discuss in more detail.

4.4.1 Effect of Parameter Variation on Device Performance

On the basis of maximum power coupling in first mirror image that is desired at wavelength 1.55 μm, the optimum waveguide height h, width w and gap between the waveguide g is choosen. The influence of power coupling with variations in waveguide height h , w at different gap as shown fig:4.5, 4.6 and 4.7

Coupling operation may be achieved by changing the transmission properties of the waveguide .this can be done by varying the gap between the waveguide and applied voltage. Form our previous discussion when waveguide bring closer together coupling between the waveguides coupling between the waveguides are increased. The quicker transfer of energy is reported due to increased coupling between the waveguide and results shorter incomplete mirror and self image, what we refer to as partial images. But when the gaps between the waveguides are increased and reach at critical point, consistent periodic transfers of power between waveguides take place and form complete mirror and self images. It is notable from fig: 4.5 that 0.07 μm is a critical gap between waveguides where after it complete images are formed and before it partial image are present, when no voltage is applied. With the application of 1 volt across the device, the effective index of the waveguide changes due to electro–optic effect result in changes the coupling between the waveguides. At gap 0.05 μm for partial images maximum coupling are reported. Therefore it is observed that optimal value of gap for partial image revival and complete image are 0.05 μm and 0.07 μm respectively.

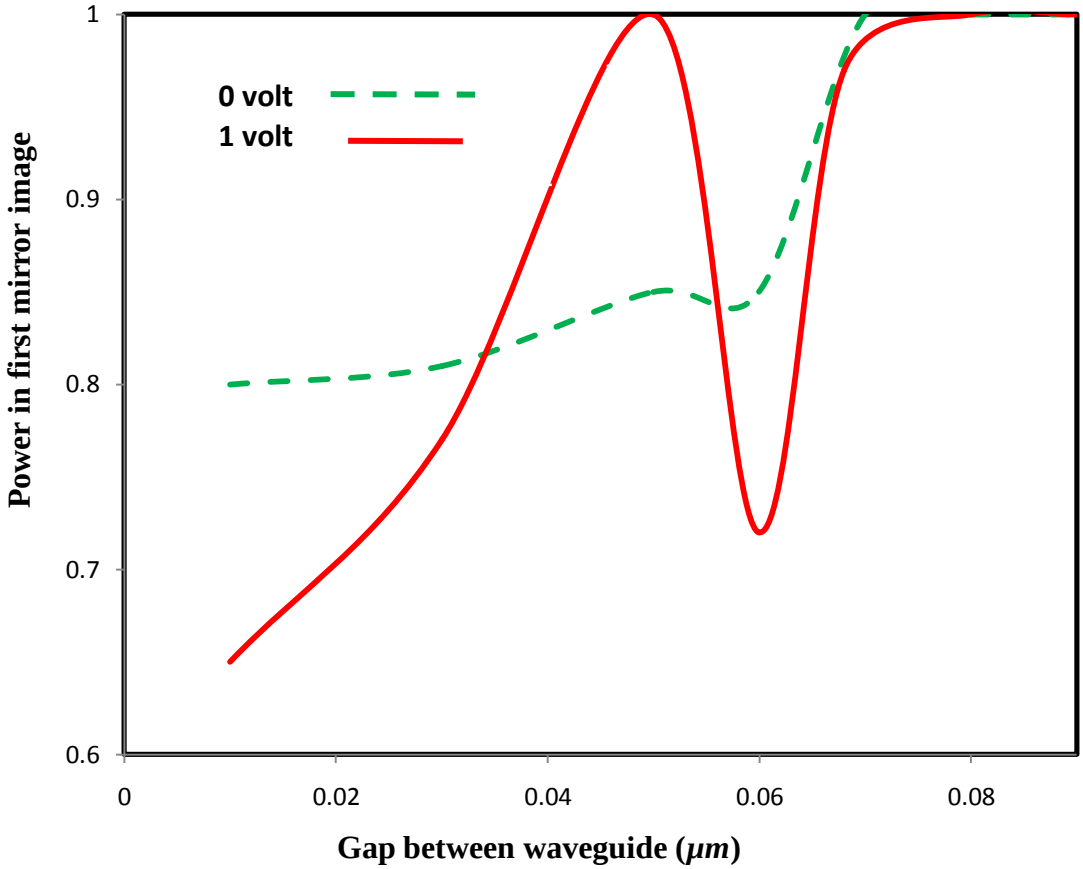

Fig: 4.5 Coupled power in second waveguide for first mirror image versus gap g between waveguides at 0 and 1 volt with variation in g from 0.01 μm to 0.09 μm

The relation between the normalized coupling power and the waveguide height h and width w with varying separation g between the waveguides is analysed. Fig: 4.6 depicts the performance of waveguide coupler at different height h .We find that with narrower the height, small power gets couple. When we future increases the height up to 0.5 μm the coupling power show almost parabolic nature. At h =0.3 μm, 80% of power get coupled to the second waveguide for gap 0.05 μm,and at the same height max. power get coupled for gap 0.07 μm. with further increase in h coupling power show a dip as seen from fig: 4.6. SOI coupler with waveguide height h, =0.3 for the gap 0.05 μm and 0.07 μm posses the maximum power coupling, hence it must be chosen.

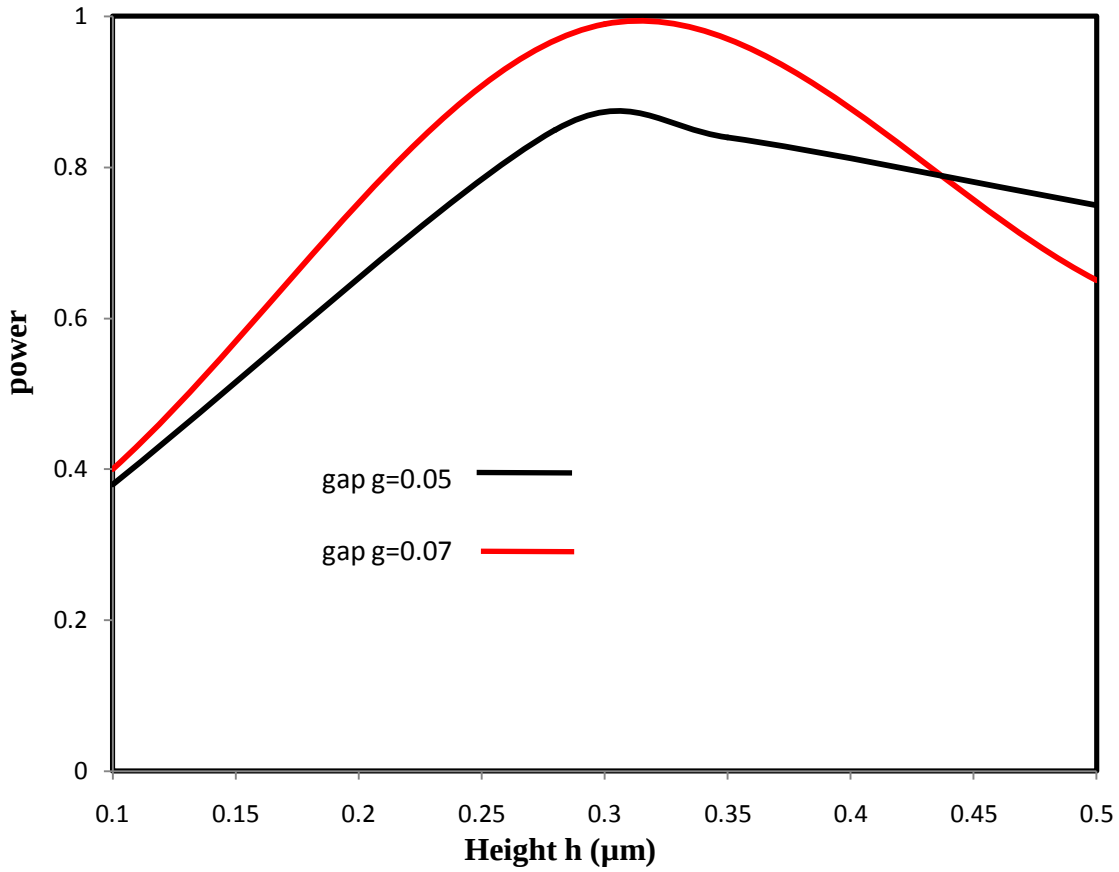

Fig: 4.6 Results of power coupling at wavelength, λ=1.55µm for the variations of waveguide height h with gap g =0.05 and 0.07 µm between the waveguides

Waveguide width w, also plays a vital role on increasing the coupling power between the waveguides. If w is chosen to be in range less than 0.5 μm, mode overlap between waveguides will not be good for gap 0.05 μm and 0.07 μm. w should be near about 0.575 μm, as either increase or decrease in its dimensions reduces the confinement of power in second waveguide, hence decreases the coupling strength. At lower w up to 0. 3 μm, less than 40 % of power is coupled, and similarly increasing the dimensions of w over 0.600 μm also don't provide the required maximum coupling strength. For the optimal value of h=0.3 μm and g=0.05 μm,0.07 µm as selected form Fig.4.5 and 4.6, coupling power of less than 60% is obtained for w in range from 300nm to 400nm. For w in range 0.400 μm to 0.595 μm, power coupling shows a steep rise toward its maximum value from initial strength of less than 25% as can be seen from Fig.4.7. When w is taken more than 600nm, power coupling will again start decreasing towards minimum value. Therefore an optimal

value of w should be selected which here is taken as 0.575 μm at h=0.3 μm & g=0.05 μm and0.07 μm,(reported from Fig.4.5), for $\lambda = 1.55$ μm as being seen from the Fig.4.7 so that maximum power get coupled.

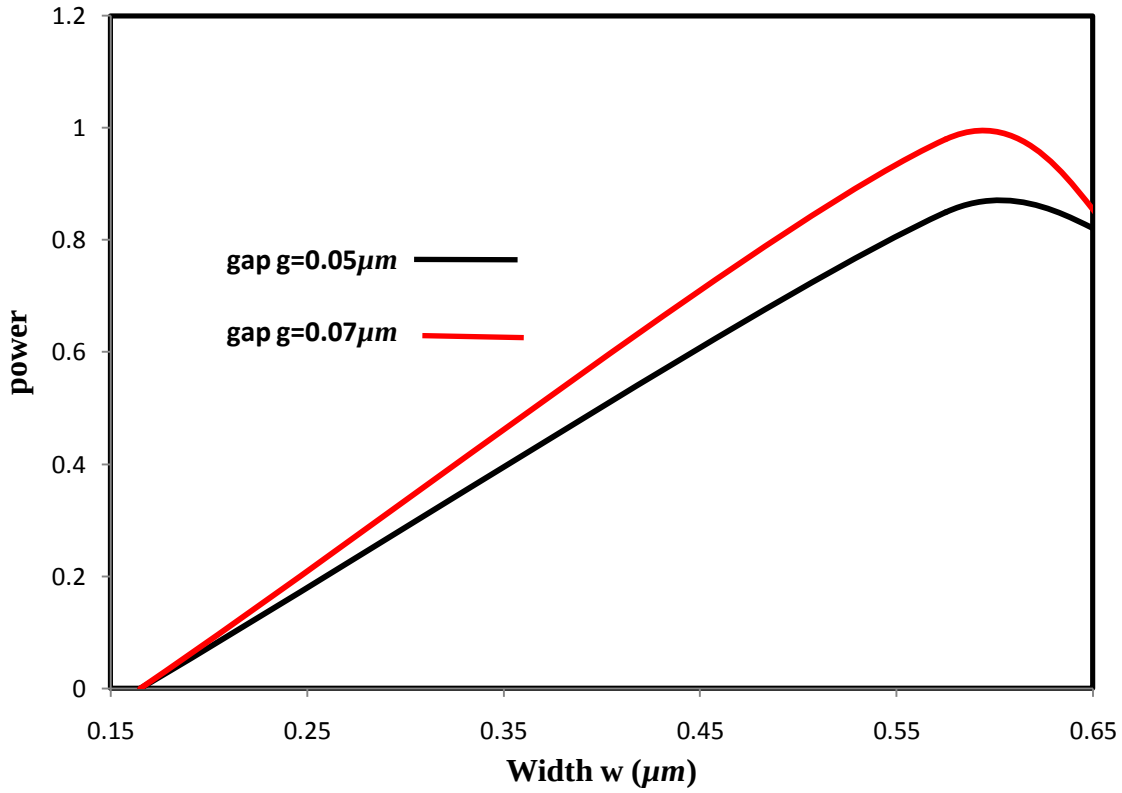

Fig : 4.7 Results of power coupling at wavelength, λ=1.55μm for the variations of waveguide width w with gap g =0.05 μm and 0.07 μm between the waveguides

4.4.2 Performance Analysis of Device with Variable Voltage

Electro–optic waveguide coupler is a potential candidate to realize active waveguide devices because of the large tuning in propagation constant (effective index) with a variable applied voltage. The device is based upon forward bias PIN junction employed carrier plasma dispersion effect, made up of SOI Rib waveguides can be a promising platform on which various tunable functionalities (switching length, power, time) can be made which may include optical switch. High speed optical switch is an important device for optical communication systems. Switching speed of optical switch depends on switching length. Fig 3 shows tuning in coupling length at different g for partial images of the proposed design with the application of voltage. Reduction in coupling length of

37.8μm to 7.7μm for gap g=0.05μm are reported from fig: 4.8 with simple tuning scheme and single tuning parameter of variable voltage. The voltage has been varied from 0 to 1 volt.

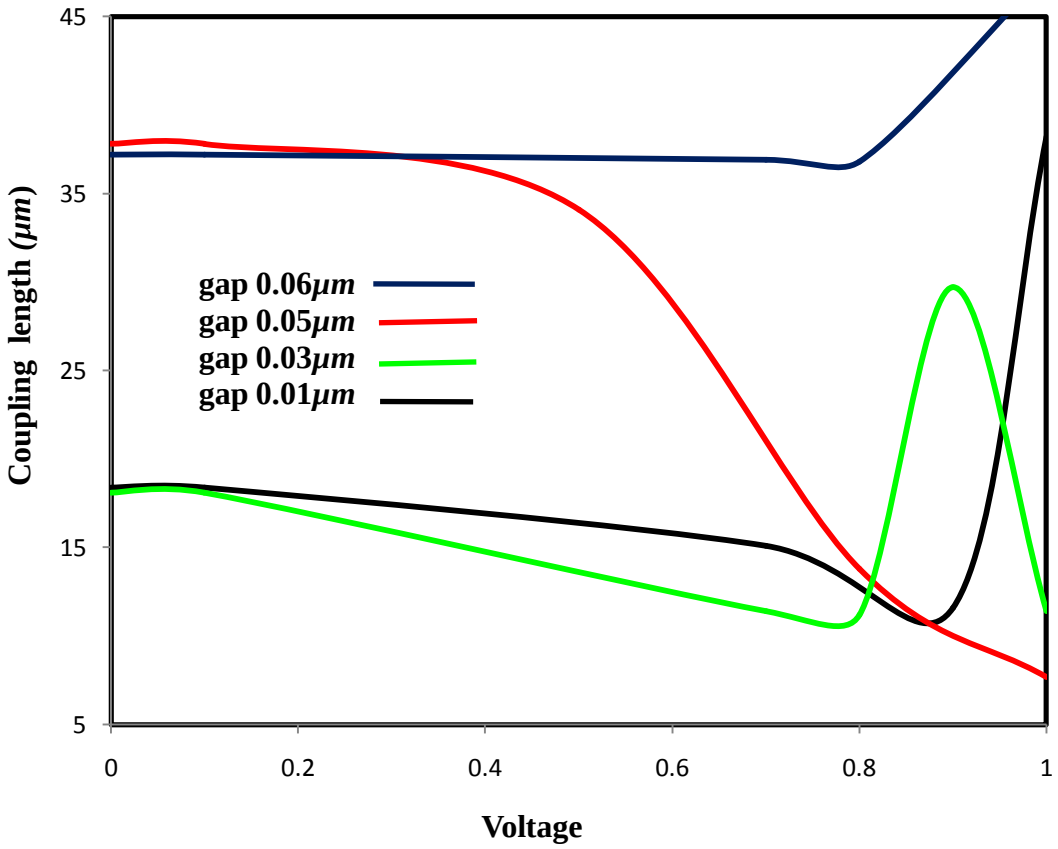

Fig:.4.8 Tuning in coupling length between the waveguide for partial images at gap g =0.01μm(black), 0.03 μm(green),0.05 μm(red) and 0.06 μm(blue) with a variation in voltage from 0 to 1 volt

Tuning in coupling length for complete images are shown in fig 4.9 Coupling length of 27.48μm is achieved at 1 volt. It can be noticed that four times reduction in coupling length on a change in voltage across the device for partial image than that for complete images. A variable voltage changes the effective index of the waveguides which in turns change the coupling between the waveguide and hence switching length has been changed. That is how a tunable waveguide coupler can be realized with Si based on PIN junction.

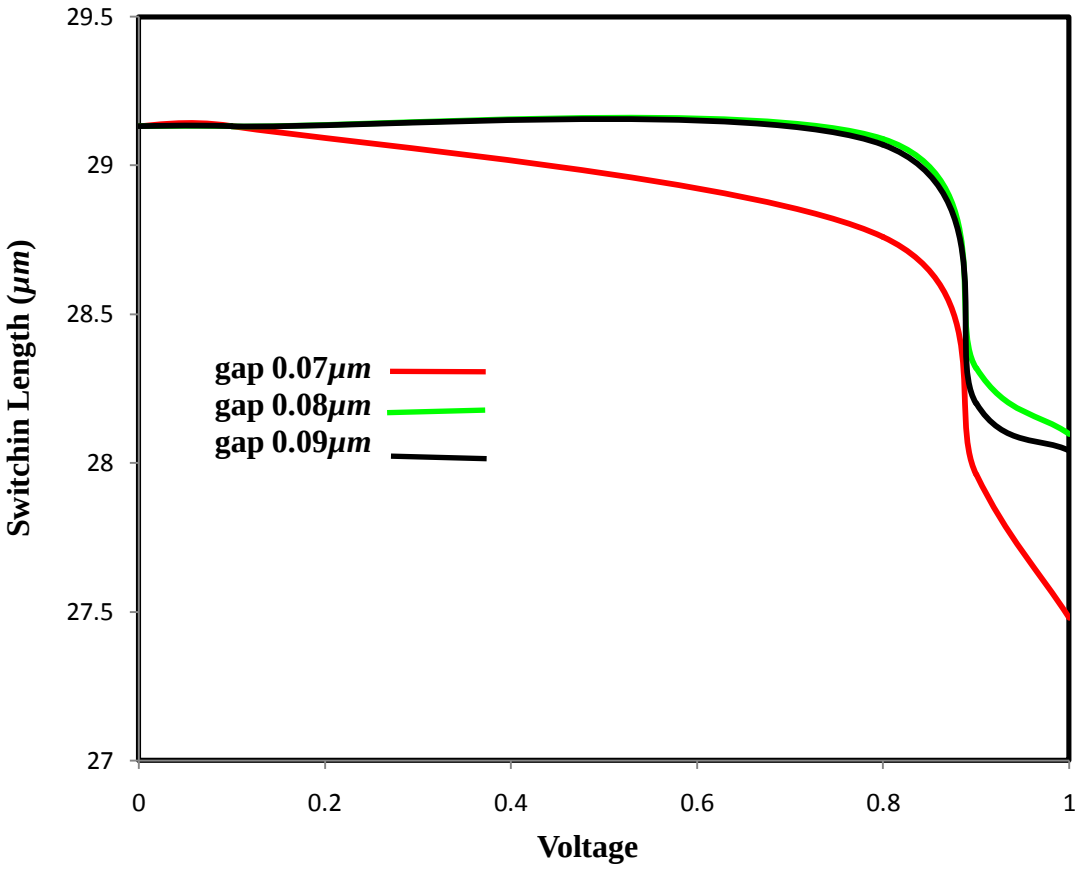

Fig: 4.9 Tuning in coupling length between the waveguide for complete images at gap g =0.09μm(black), 0.08 μm(green) and 0.05 μm(red)) with a variation in vo--tage from 0 to 1 volt

4.4.3 Comprative Analysis of Coupling Length

Integrating the optimized values of g =0.05μm and 0.07μm (partial image and complete image respectively) ,w=0.575μm,h=0.3μm switching characterstics of device are shown in images 4.10 (a),(b)and (c).The simulated power evolution for a two channel waveguide illustrates a consistent periodic mirror- and self-image phenomenon when no voltage is applied across the device. These figures indicate that the mirror-images and self-images are complete image revivals of the input field, at this stage the coupling length L_{c1} is reported 29.132μm for complete image from fig: 4.10(a).

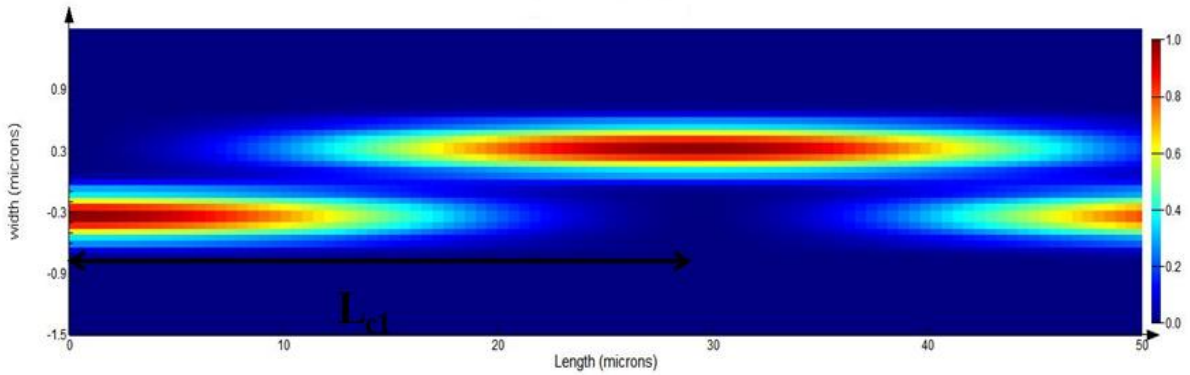

(a)

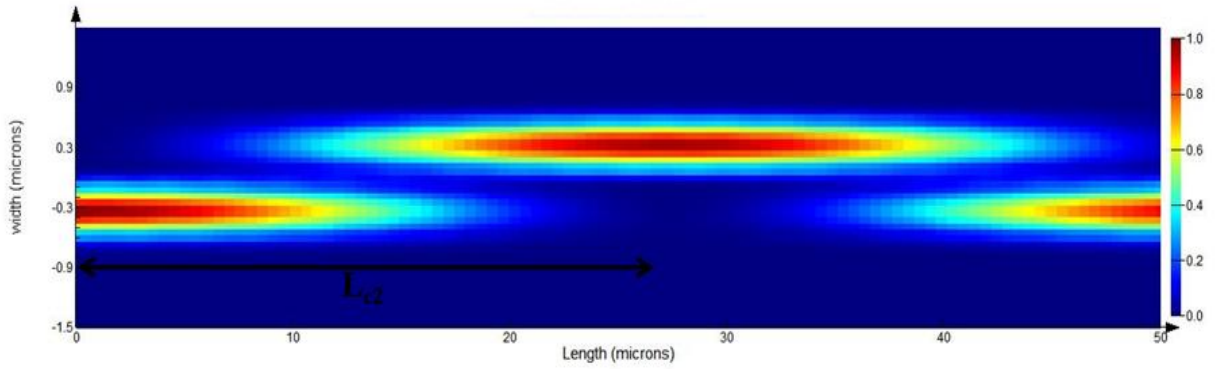

(b)

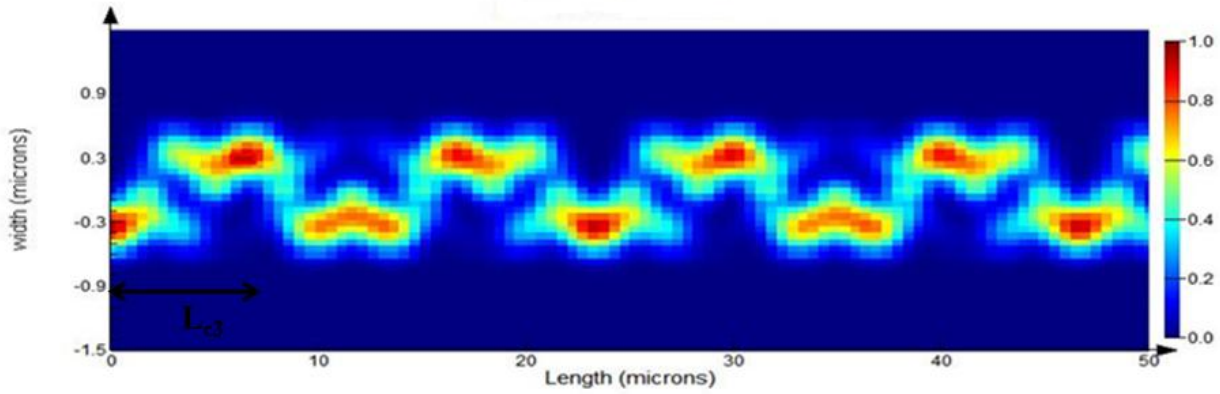

(c)

Fig 4.10 Simulated optical power intensity evolution of a electro-optic waveguide coupler for an applied voltage of (a) 0 V; and (b) 1V (c).1V showing coupling length L_{c1} L_{c2} and L_{c3} respectively.

With the application of 1V across the device, the refractive index changes due to the electro-optic effect result in changes to the propagation constants. Consequently, this changes the multi-mode interference pattern, that forms between the supermodes resulting in changes to the imaging points along the device as shown in Fig:4.10 (b). Which results the reduction in coupling length of about 1.06 times and give a coupling length L_{c2}= 27.48μm

When waveguide bring closer together i.e. gap between the waveguide reduced to 0.05 μm coupling between the waveguides are increased. The quicker transfer of energy is reported due to increased coupling between the waveguide and results shorter incomplete mirror and self image, what we refer to as partial images as shown in Fig:4.10(c). Simulated optical power intensity evolution at 1 volt for partial image waveguide coupler reports the coupling length L_{c3} equal to 7.7μm. It is noticed that the coupling length L_{c3} for partial images is approximately four times smaller than that of complete images coupling length $L_{c1.}$

Chapter 5

Conclusion and Future Scope

This work focuses on the design and analysis of electronically tunable waveguide coupler on SOI with a small coupling length. The analysis is presented on the basis of Multi-mode Interference and principal of self imaging. In a wave guide coupler, on bringing the waveguides closer, waveguide coupling increases which results in a quicker transfer of energy between the waveguides. This forms a more complex interference pattern with shorter mirror- and self-image lengths. This result is the formation of what we refer to as partial image revivals at periodic intervals along the direction of propagation of the device. We now have the advantage of the increased coupling and hence shorter image lengths. In order to illustrate the use of this phenomenon, an integrated waveguide coupler is designed based on carrier plasma dispersion in silicon; The optimized device-parameters are: gap between waveguides g = 0.05 μm, waveguide height h = 0.3 μm and width w = 0.575 μm. With the application of 1 volt across the proposed design, waveguide refractive index changes as a function of free carrier concentration and causes the reduction in coupling length up to 7.7 μm while the reduction in coupling length from 29.13 μm to 27.48 μm is reported for complete at optimum gap g = 0.07 μm. It is noticed that the coupling length for partial images is approximately four times smaller than that of complete images for 1 volt at the expanse of shorter image.

As a general conclusion, the electronically tunable waveguide coupler on SOI is a promising approach for enabling high speed sub micrometer size active waveguide devices on Si which can be a building block for realization of compact optical modulator based on silicon photonics. For the present level of competence in integrated optics it is possible that large number of these elements can be used to constitute multi channel waveguide coupler for practical applications in high density switches and modulators. The next recommended effort may focus on achieving the further small coupling length for voltage exceeding 1 volt.

Chapter 7

References

[1] H.Chul, H. Kim, and Y.Chur, "Full-Duplex Radio- Over-Fiber System Using Phase Modulated Downlink and Intensity-Modulated Uplink", *IEEE Photon. Techno. Lett.* Vol. 21, No.1 (2009), pp. 9-11.

[2] H. B. Kim, H. Woesner, and A. Wolisz, "A Medium Access Control Protocol for Radio Over Fiber Wireless LAN Operating in the 60-GHz Band", *5th European Personal Mobile Comm. Conf. (EPMCC)*, (2003).

[3] Jianping Yao, "Microwave Photonics", *Journal. of Lightwave Technology*, Vol. 27, No. 3 (2009), pp. 314-335.

[4] Hong Ma, Alex K.Y. Jen, and Larry R. Dalton, "Polymer-Based Optical Waveguides: Materials, Processing, and Devices", *Advanced Materials*, Vol.14, No.19 (2002), pp.1339-1365.

[5] Louay Eldada, "The Promise Of Polymers", *SPIE's OE Magazine* (2002) *pp. 26- 29*.

[6] Changming Chen, Feng Zhang, Hui Wang, Xiaoqiang Sun, Fei Wang, Zhanchen Cui, and Daming Zhang, "UV Curable Electro-Optic Polymer Switch Based on Direct Photodefinition Technique", *IEEE Journal Of Quantum Electronics*, Vol. 47, No**. 7**, (2011) pp-959-964.

[7] Ajoy Ghatak, k.thyagarajan , "Optical Electronics," *Cambridge University Press*, ISBN 81-85618-100 2010.

[8] B. Jalali, S. Yegnanarayanan, T. Yoon, T. Yoshimoto, I. Rendina, and F. Coppinger, "Advances In Silicon-On-Insulator Optoelectronics", *IEEE Journal Selected Topics Quantum Electronics*, Vol. 4, No. 6(1998), pp. 938–947.

[9] R. C. Johnson,"Intel Reveals Long-Term Goals For Silicon Photonics Sensors", Electronics Eng. Times [Online]. http:// www.eetimes.com/semi/news/OEG20020228S0033, (2002).

[10] L. C.Kimerling, "Photons To The Rescue: Microelectronics Becomes Microphotonics", *Electrochem. Soc. Interface*, (2000) p. 28.

[11] Abd El–Naser A. Mohamed, Mohamed A. Metawe'e , Ahmed Nabih Zaki Rashed, and Amira M. Bendary ," Recent Progress of LiNbO3 Based Electrooptic Modulators with Non Return to Zero (NRZ) Coding in High Speed Photonic Networks", *International Journal of Information and Communication Technology Research*, Vol. 1, No. 2 (2011), pp 55-63.

[12] Hirotoshi Nagata, Junichiro Ichikawa,"Progress and Problems in Reliability of Ti:LiNbO3 Optical Intensity Modulators ," *Optical Engineering* ,Vol. 34 , No. 11(1995) pp 3284-3293.

[13] G. T. Reed, A. P. Knights, "Silicon Photonics: an introduction", John Wiley, Chichester (2004).

[14] Robert Goldstein "Electro-Optic Devices in Review," *Lasers and Applications* (1995), pp1-6 l.

[15] Sun Xiao-Qiang, Chen Chang-Ming, LI Xiao-Dong, Wang Xi-Bin Yang Tian-Fu, Zhang Da-Ming, Wang Fei,Xie Zhi-Yuan , "Polymer Electro-optic Modulator Linear Bias Using the Thermo-optic Effect", *Chin. Phys. Lett.*,Vol. 29, No.1(2012), pp 1-4.

[16] Joris Van Campenhout, William M. J. Green, Solomon Assefa, and Yurii A. Vlasov "Ultra-Broadband, Low-Power, 2x2 Electro-Optic Switch using Sub-Micron Silicon Waveguides", *OSA / OFC/NFOEC*(2010), pp. 844-847.

[17] Bradley Schmidt, Qianfan Xu, Jagat Shakya, Sasikanth Manipatruni, and Michal Lipson, "Compact Electro-Optic Modulator on Silicon-on Insulator Substrates Using Cavities With Ultrasmall Modal", *Optics Express*, Vol. 15, No. 6 (2007), pp. 3140-3148.

[18] A. Llobera, V. Seidemann, J. A. Plaza, V. J. Cadarso, and S. Büttgenbach, "Integrated Polymer Optical Accelerometer" *IEEE Photonics Technology Lett.*, Vol. 17, No. 6(2005), pp. 1262-1264.

[19] Richard Syms ,John Cozens, "Optical Guided Waves And Devices" McGraw-Hill, New York, ISBN 0-07-707425-4(1992) , pp. 200-450.

[20] Nishihara, H. M. Haruna, and T. Suhara ,"Optical Integrated Circuits", McGraw-Hill, New York(1989), pp. 456-500.

[21] Y.Enami, D.Mathine, C.T.DeRose, R.A.Norwood, J.Luo, A.K.Y.Jen, and N. Peyghambarian1 "Hybrid Electro-Optic Polymer/Sol-Gel Waveguide Directional Coupler Switches" *Applied physics letters*, Vol. 94(2009), pp. 1-4.

[22] H. Kogelnik and R. V. Schmidt, “Switched Directional Coupler With Alternating Δβ”, *IEEE Journal. Quantum Electron.*, Vol. QE-12(1976), pp. 396-401.

[23] R. A. Forver and E. Marom, “Symmetric Directional Coupler Switches”, *IEEE Journal Quantum Electron.*, Vol. QE-22(1986), pp. 911-919.

[24] L. Lierstuen and A. Subdo, “8-Channel Wavelength Division Multiplexer Based on Multimode Interference Couplers”, *IEEE Photon. Technol. Lett*., Vol. 7, No. 9(1995), pp. 1034–1036.

[25] N. Agrawal, C. Weinert, H. Ehrke, G. Mekonnen, D. Franke, C. Bornholdt, and R. Langehorst, “Fast 2x2 Mach–Zehnder Optical Space Switches Using InGaAsP–InP Multi Quantum-well Structures”, *IEEE Photonics Technol. Lett*., Vol. 7, No. 6(1995), pp. 644–645.

[26] Peter Hertel ,“Dielectric Waveguides”, *Optics Letters*(2009), pp 25-40

.

[27] Yaocheng Shi, “ Design, Simulation And Characterization Of Some Planar Lightwave Circuits”, Doctoral Thesis, KTH School of Information and Communication Technology SWEDEN, ISSN 1653-7610, ISBN 97 -91-7178-989-1(2008).

[28] Y. Sun, X. Jiang, J. Yang, Y. Tang, and M.Wang, “Experimental Demonstration of 2-D MMI Optical Power Splitter”, *Chin. Phys. Lett*., Vol. 20(2003), pp. 2182–2184.

[29] Y. Tang, W. Wang, Y. Wu, J. Yang, and Y. Wang, “Multimode Interference Coupler with Strong Confinement Structure on Silicon on-Insulator”, *Opt. Eng.*, Vol. 43(2004), pp. 2495–2496.

[30] Bahaa E. A. Saleh, Malvin Carl Teich "Fundamentals Of Photonics", John Wiley & Sons, ISBNs: 0-471-83965-5 (Hardback); 0-471-2-1374-8 (Electronic) (1991)

[31] Henry F. Taylor and Amnon Yariv, "Guided Wave Optics" ,Proc. of the IEEE, Vol. 62, No. 8(1974), pp1044-1060.

[32] H. A. Haus, W. P. Huang, S. Kawakami, and N. A. Whitaker ,"Coupled-Mode Theory of Optical Waveguides", *Journal Of Lightwave Technology*, Vol. LT-5, No. 1(1987), pp16-23.

[33] A. Yariv, "Coupled-mode Theory for Guided-wave Optics", *IEEE Journal Quantum Electronics*, Vol. QE-9(1973), pp. 919-933.

[34] R. R. A. Syms, "Improved Coupled-Mode Theory for Codirectionally and Contradirectionally Coupled Waveguide Arrays", *Journal Opt. Soc. Am.*,Vol. 8, No. 7(1991), pp. 1062-1069

[35] G. T. Paloczi, Y. Huang, A. Yariv, J. Luo, and A. K.-Y. Jen, "Replicamolded Electro-Optic Polymer Mach–Zehnder Modulator", *Appl. Phys.Lett.*, Vol. 85, No. 10(2004), pp. 1662–1664.

[36] Gerhard Hagn, "Electro-Optic Effects and Their Application in Indium Phosphide Waveguide Devices for Fibre Optic Access Networks", Doctoral Thesis, Swiss Federal Institue of Technology Zürich (2001).

[37] F.Y Gardes, G.T.Reed, A.P Knights, G .Mashanovich , "Evolution of Optical Modulation using Majority Carrier Plasma Dispersion Effect in SOI", *Proc. of SPIE,* Vol. 6898, 68980C(2008), pp. 1-9.

[38] Brian R. Bennett, Richard A. Soref and Jesus A. Del Alamo, "Carrier-Induced Change in Refractive index of GaAs, and InGaAsP", *IEEE Journal of Quantum Electronics,* Vol. 26, No. 1(1990), pp 113-122.

[39] R. A. Soref and B. R. Bennett, "Electro-optical Effects in Silicon," *IEEE Journal Quantum Electron.,* Vol. QE-23, No. 1(1987), p. 123.

[40] C. Z. Zhao, A. H. Chen, E. K. Liu, and G. Z. Li, "Silicon-on-Insulator Asymmetric Optical Switch Based on Total Internal Reflection", *IEEE Photon. Technol. Lett*., Vol. 9, No. 8(1997), p. 1113.

[41] Y.A.Vlasov and S.J.McNab, "Losses in Single-mode Silicon-on-Insulator Strip Waveguides and Bends", *Opt. Express,* Vol. 12, No. 8(2004), pp. 1622–1631.

[42] P. D. Trinh, S. Yegnanarayanan, F. Coppinger, and B. Jalali, "Silicon-on-insulator (SOI) Phased-Array Wavelength multi/multiplexer with Extremely Low-Polarization Sensitivity",. *IEEE Photon. Technol. Lett.,* Vol.9, No.7(1997), pp 940-942.

[43] W. Lukosz, K. Tiefenthaler, "Directional Switching in Planar Waveguides Effected by Absorbtion–Desorbtion Processes", *IEEE 2nd European Conference of Integrated Optics,* Vol. 227, Florence, Italy(1983), pp. 152–155.

[44] P. Kaczmarski, J.P.Van de Capelle, P.E. Lagasse ,R. Meynart, "Design of an Integrated Electro-Optic Switch in Organic Polymers", *IEE Proc*., Vol. 136, No. 3, (1989),pp. 152-158.

[45] Wei Yu Lee, Jin Shin Lin, and Sung Yuen Wang ,"A Novel Vertical ΔK Directional Coupler Switch Using Liquid Crystals", *Journal Of Lightwave Technology*, Vol. 13, No. 1(1995), pp. 49-54.

[46] Lucas B. Soldano and Erik C. M. Pennings, "Optical Multi-Mode Interference Devices Based on Self-Imaging : Principles and Applications", *Journal Of Lightwave Technology*, Vol. 13, No. 4(1995), pp. 615-627.

[47] R. Chakraborty, J.C. Biswas, S.K. Lahiri, "Analysis of Directional Coupler Electro-Optic Switches using Effective-index-Based Matrix Method", *Optics Communications* Vol. 219 (2003), pp. 157–163.

[48] C. Angulo Barrios, V. R. Almeida, "Electrooptic Modulation of Silicon-on-Insulator Submicrometer-Size Waveguide Devices", *Journal of Lightwave Technology*, Vol. 21, No. 10(2003), pp. 2332-2339.

[49] Kjersti Kleven and Scott T. Dunham, "Design And Simulation Of A Hybrid Silicon/ Electro-Optic Polymer Modulator" *NUSOD* (2005), pp .49-50.

[50] Fan Wang, Jianyi Yang, Limei Chen, Xiaoqing Jiang, and Minghua Wang, "Optical Switch Based on Multimode Interference Coupler", *IEEE Photonics Technology Lett.* Vol. 18, No. 2(2006), pp. 421-423.

[51] Abdulaziz Mohammed Al-Hetar, Abu Bakar Mohammad, Abu Sahmah M. Supa'at, and Zaid Ahmed Shamsan, "MMI-MZI Polymer Thermo-Optic Switch With a High Refractive Index Contrast", *Journal Of Lightwave Technology,* Vol. 29, No. 2(2011), pp 171-177.

[52] Ansheng Liua, Ling Liaoa, Doron Rubinb, Hat Nguyena, Berkehan Ciftcioglua, Yoel Chetritb, Rami Cohenb, Nahum Izhakyb, Juthika Basaka, and Mario Panicciaa, "Recent Advances in High Speed Silicon Optical Modulator," *Proc. of SPIE,* Vol. 6477(2007) , pp. 1-9.

[53] Chuan-Tao Zheng, Chun-Sheng Ma, Xin Yan, Xian-Yin Wang, Da-Ming Zhang "Simulation and Optimization of a Polymer Directional Coupler Electro-Optic Switch with Push–Pull Electrodes" *Optics Communications,*Vol. 281(2008) ,pp. 3695–3702 .

[54] S.Ponmalar, S.Sundaravadivelu, "Design of Ultra Fast Polymer Electro-Optic waveguide Switch for Intelligent Optical Networks" *International Journal of Electrical and Computer Engineering,* Vol. 4, No. 8(2009), pp. 543-547.

[55] R. J. Mc Cosker and G. E. Town, "Partial Image Revivals In A Multichannel Directional- Coupler*", Proc. SPIE,* Vol. 7604, 76040 G,(2010)

[56] Po Dong,Shirong Liao,Hong Liang, Roshanak Shafiiha, Dazeng Feng, Guoliang ,Li Xuezhe Zheng, Ashok V. Krishnamoorthy, and Mehdi Asghari, "Submilliwatt, Ultrafast and Broadband Electro-Optic Silicon Switches", *Optics Express* Vol. 18, No. 24(2010), pp. 25225-25231.

[57] Ravi J. McCosker and Graham E. Town," An Electro-Optic Modulator using a Multi-Channel Directional Coupler with a Poled Electro-Optic Polymer",

International Conference on Electromagnetic in Advance Application-ICEAA(2011), pp 329-334.

[58] Antao Chen, Haishan Sun, Attila Szep, Shouyuan Shi, Dennis Prather, Zhou Lin, Richard S. Kim, and Don Abeysinghe, "Achieving Higher Modulation Efficiency in Electrooptic Polymer Modulator With Slotted Silicon Waveguide", *Journal Of Lightwave Technology*, Vol. 29, No. 21(2011), pp. 3310-3318.

[59] Qiliang Li, Aixin Zhang, Xiaofeng Hua, " Numerical Simulation of Solitons Switching and Propagating in Asymmetric Directional Couplers", *Optics Communications,*Vol. 285(2012), pp. 118–123.

[60] Kenjal jain, Prof. H.K.Dixit, "Optimization of 2x2 Mach-Zehnder Interferometer Electro-Optic Switch", *Third International Conference on Computer and Communication Technology* (2012), pp 171-174.

[61] R.W. Chuang, M.T.Hsu, Y.C. Chang, Y.-J. Lee, S.H. Chou, "Integrated Multimode Interference Coupler-Based Mach–Zehnder Interferometric Modulator Fabricated on a Silicon-on-Insulator Substrate", *IET Optoelectron.*, Vol. 6, No. 3(2012), pp. 147–152.

[62] Eric F. Dudley and Wounjhang Park, "Ultra-Compact High-Speed Electro-Optic Switch Utilizing Hybrid Metal-Silicon Waveguides", *Journal of Lightwave Technology*, Vol. 30, No. 21(2013), pp. 3401-3406.

[63] Shiyang Zhu, G. Q. Lo, and D. L. Kwong ," Ultracompact Si Electro-Optic Modulator Based on Horizontal Cu-Insulator-Si-Insulator-Cu Nanoplasmonic Waveguide," *OFC/NFOEC Technical Digest OSA* (2013).

[64] Hui Yu, Marianna, Pantouvaki, Sarvagya Dwivedi, Peter Verheyen, Guy Lepage, Roel Baets, Wim Bogaerts, Philippe Absil, and Joris Van, "Compact Thermally Tunable Silicon Racetrack Modulators Based on an Asymmetric Waveguide", *IEEE Photonics Technology Lett.*, Vol. 25, No. 2(2013), pp. 159-162.

[65] Ravi J. McCosker, Graham E. Town, "Multi-channel directional coupler as an evanescent field optical sensor," *Sensors and Actuators B 150* ,(2010),pp. 417–424,

[66] University of California, San Diego Micro/Nano-Photonics Group"device for computing" http://mnp.ucsd.edu/optical, (2012).